Polyhedron 242 (2023) 116487

Contents lists available at ScienceDirect

Polyhedron

journal homepage: www.elsevier.com/locate/poly

Synthesis of novel Cu(II) complexes with N_2O_2 ligands: Characterization, theoretical calculations, antimicrobial, antioxidant, DNA binding, and in vitro anticancer activity studies

Arif Mermer [a,b,c,*], Burak Tüzün [d], Sevgi Durna Daştan [e], Özge Çevik [f]

[a] Experimental Medicine Application and Research Center, University of Health Sciences-Turkey, Uskudar 34662, Istanbul, Turkey
[b] Department of Biotechnology, University of Health Sciences-Turkey, Uskudar 34662, Istanbul, Turkey
[c] UR22722, LABCİS, Faculty of Science and Technology, University of Limoges, F-87000 Limoges, France
[d] Plant and Animal Production Department, Technical Sciences Vocational School of Sivas, Sivas Cumhuriyet University, Sivas, Turkey
[e] Department of Biology, Faculty of Science, Sivas Cumhuriyet University, Sivas, Turkey
[f] Department of Biochemistry, Faculty of Medicine, Adnan Menderes University, Aydın, Turkey

ARTICLE INFO

Keywords:
Antimicrobial
Antioxidant
Cytotoxicity
DNA interaction
Molecular docking
ADME/T

ABSTRACT

The aim was to investigate the in vitro antimicrobial, antioxidant, cytotoxic activities and pBR322 Plasmid DNA interaction potentials of newly synthesized Schiff bases and their copper complexes. Cytotoxic activities of these compounds were determined by MTT methods in human breast cancer (MCF-7), human cervical cancer (HeLa) and mouse fibroblast (L929) cell lines. The determination of changes in oxidant and antioxidant load of the cell after application of these compounds were investigated with the aid of Rel Assay Diagnostics kits. It was found that the some of the compounds had moderate antimicrobial activity, and oxidative stress index. According to plasmid DNA interaction studies, synthesized complexes modified the tertiary structure of pBR322 plasmid DNA. The compound **Bis-Napht** showed the highest cytotoxic activity in HeLa, MCF-7 and L929 cells at an IC50 dose of 3 ± 1 μM, 5 ± 1 μM and 3 ± 1 μM respectively. Compound **Bis-Sal** was determined to have lower cytotoxic activity in L-929 cells at an IC50 dose of 106 ± 9 μM at 24 h compared to other compounds. Ligand compounds and their metal complexes were optimized on the B3LYP, HF, and M06-2x methods with the 6–31++g(d,p) basis set. Afterwards, their activities were compared against crystal structure of the BRCT repeat region from the breast cancer associated protein, (BRCA1) (PDB ID: 1JNX) and crystal Structure of CDK2 receptor of cervical cancer cell proteins (PDB ID: 4BGH). To examine the interactions occurring in more detail, Protein-Ligand Interaction Profiler analysis was performed and all chemical interactions that occurred were determined.

1. Introduction

Schiff bases and their metal complexes, which have numerous advantages, are considered an important class of compounds that are widely studied due to their chemical, biochemical and electrochemical properties [1–4]. Schiff base ligands are characterized by the formation of an imine bond by the condensation of an amino and carbonyl compounds [5]. These compounds are mono or polydentate systems that include different donor sites and able to coordinate several transition metal ions by coordinative interactions with some or the entire donor atoms present in the molecular structure [6–8].

The copper ion, which is an important trace element in the human body and has biological properties, plays a critical and significant place in both many biological processes, enzyme regulation, and in the structural and functional development of proteins [9]. Further, it has been displayed to have redox features suitable for the formation of complexes that damage DNA efficiently, and because of being fourth period element, it is remarkably less toxic to humans than higher period elements such as platinum [10]. Thus, copper complexes derived from Schiff base ligands were selected as excellent starting points to achieve the main aim of this study.

Cancer is one of the important health problems with increasing incidence and limited treatment options [11,12]. Due to the inadequacy of the methods and drugs used in cancer treatment, the serious side effects and cost of treatment methods, studies on synthesizing effective compounds in cancer treatment are intensified [13,14]. Breast cancer is

* Corresponding author at: Experimental Medicine Application and Research Center, University of Health Sciences-Turkey, Uskudar 34662, Istanbul, Turkey.
E-mail address: arif.mermer@sbu.edu.tr (A. Mermer).

https://doi.org/10.1016/j.poly.2023.116487
Received 27 February 2023; Accepted 1 June 2023
Available online 13 June 2023

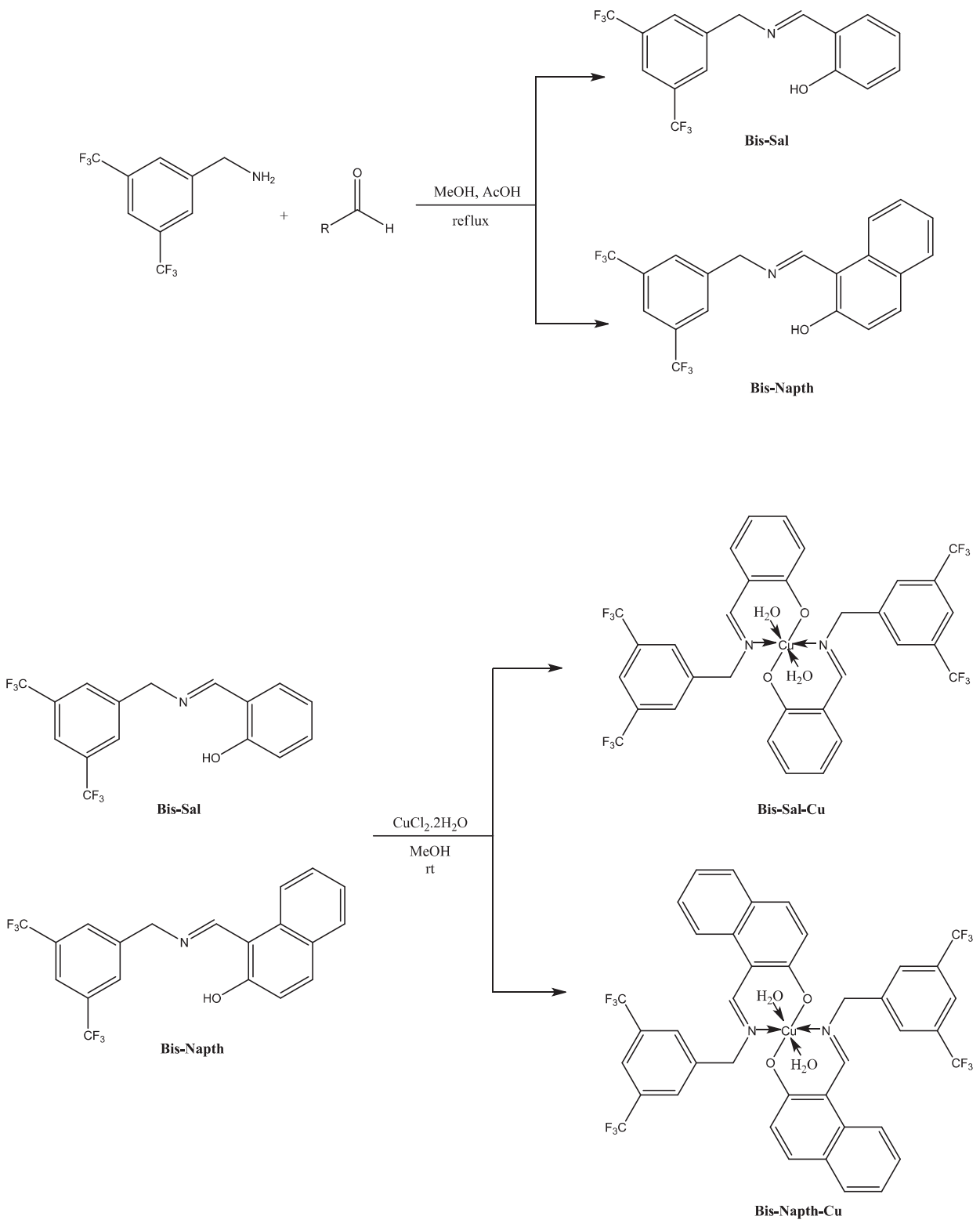

Scheme 1. Synthesis of Schiff bases and their copper complexes.

one of the most common cancer types, accounting for >18% of all cancers. Differential responses among individuals in breast cancer pathology, it is difficult to treat because there are different classes of tumors that exhibit and this type of cancer among women leading cause of death. The MCF 7 cell line is a suitable model cell line for breast cancer. It is preferred worldwide in anticancer activity studies and drug design studies. Cervical carcinoma is also one of the common cancers in women. The papilloma viruses play a significant-causative roles in the development of this disease and surgery, chemotherapy, hormonal therapy, radiation therapy are effective treatment methods [15]. The patients treated with chemotherapy are exposed to treatment-related sudden and long-term toxicities. Chemotherapy is a treatment with a large number of drugs to kill cancer cells. In cases where the disease progresses, chemotherapy and radiotherapy or different

chemotherapeutic agents are used in combination. The ideal drug is expected to kill only cancer cells without harming normal cells, but this property is not present in most drugs currently used in clinical practice. Because there is not much difference in terms of quantity between malignant cancer cell and normal human cell. For these reasons, there is a need for the discovery and/or synthesis of new alternative agents for the treatment and prevention many types of cancer [14]. Toxicity studies have been carried out in cancer cell lines using anticancer drugs, different nanoparticles or various drugs [16]. Apart from examining various diseases and disease agents in detail, cell cultures are also very important in terms of developing vaccines suitable for viruses, developing tissue and gene therapies, and observing in detail the personalized treatment methods and individual drug dosing. With all these advantages they provide, cell cultures have very positive effects in health sciences, enabling the further development of today's medicine and it is believed that they will be useful in the treatment of many diseases in the future [17].

In present study, we aimed to determine the antioxidant or oxidant level-modifying properties of the compounds **Bis-Sal, Bis-Sal-Cu, Bis-Napht** and **Bis-Napht-Cu** in cells, antimicrobial activities on 4 different microbial strains, and define the cytotoxicity of these compounds on 2 different cancer cell lines and one healthy cell line. L929 cell line consisting of mouse fibroblast cells was used in our study to compare the effects of the compounds used on healthy cells. Further, in this study we report a brief overview of these compounds' ability to modify the form I and II bands of pBR322 plasmid DNA with the electrophoretic mobility. The comparison of the activities of the compounds with the theoretical calculations was made. Two different programs were used for comparison. First, ligand compounds and their metal complexes were optimized on the B3LYP, HF, and M06-2x [18–20] methods with the 6–31++g(d,p) basis set. Afterwards, their activities were compared against Crystal structure of the BRCT repeat region from the breast cancer associated protein, (BRCA1) (PDB ID: 1JNX) [21] and Crystal Structure of CDK2 receptor of cervical cancer cell proteins (PDB ID: 4BGH) [22]. In order to examine the interactions occurring in more detail, Protein-Ligand Interaction Profiler analysis [23] was performed and all chemical interactions that occurred were determined.

2. Material and methods

All commercial solvents and reagents were provided from Sigma-Aldrich and used without further purification. The progress of the reactions was followed by TLC (Thin Layer Chromatography) on silica gel 60 F254 aluminum sheets. FTIR (Fouirer Transform Infrared Spektrofotometre) spectra were recorded using a ThermoFisher Scientific Nicolet IS50 FTIR spectrometer. TGA (Thermogravimetric analysis) of compounds was performed using PerkinElmer TGA-8000 Thermogravimetric Analyzer (TGA 800). ^{1}H NMR and ^{13}C NMR (APT) spectra were recorded on Bruker Avance II 400 MHz NMR spectrometer (chemical shift in ppm downfield from TMS (tetramethylsilane) as an internal reference). The mass spectra were obtained at MALDI-TOF/MS (UltrafleXtreme, Bruker). Molar conductivity (10^{-3} mol L^{-1}) of the complexes in DMSO (dimethyl sulfoxide) were measured by the Hanna Instruments conductivity meter. Elemental analysis (C, H and N) of the synthesized compounds were performed by Leco/Truespec Micro. The FS5 Spectrofluorometer (Edinburg Instruments) was used for obtaining electronic spectra measurement. The molar magnetic susceptibilities were measured on powdered samples using Gouy method.

2.1. Synthesis of ligands

Salicyaldehyde or 2-hydroxy-1-naphthaldehyde (10 mmol) dissolved in methanol was added to 3,5-bis(trifluoromethyl)benzylamine (10 mmol) in methanol in the presence of glacial acetic acid (3–4 drops). The reaction mixture was refluxed for 6 h, and reaction progress was monitored by TLC. After completion of the reaction, the reaction mixture was concentrated under reduced pressure, and obtained yellow solid filtered, washed with cold ethanol, and dried. The crude product was recrystallized from ethanol to afford the corresponding compounds (Scheme 1). The FT-IR, ^{1}H NMR and ^{13}C NMR (APT) and MS spectra for ligands are shown in Figs. S1-S8.

2.1.1. 2-[E-({[3,5-bis(trifluoromethyl)phenyl]methyl}imino)methyl] phenol (Bis-Sal)

FT-IR (υ_{max}, cm^{-1}): 3078.22 (*ar*-H), 1633.61 (C═N), 1278.56 (C—O). ^{1}H NMR (400 MHz, DMSO-d_6, δ ppm): 4.96 (s, 1H, CH_2), 6.86–6.92 (m, 2H, arH), 7.31–7.35 (m, 1H, arH), 7.49 (dd, 1H, $J_1 = 4.0$, $J_2 = 4.0$ Hz, arH,), 7.99 (s, 1H, arH), 8.06 (s, 2H, arH), 8.75 (s, 1H, CH), 13.02 (s, 1H, OH). APT (^{13}C NMR) (100 MHz, DMSO-d_6): 61.23 (CH_2), 116.89 (CH), 119.15 (C), 119.27 (CH), 119.69 and 122.40 ($d_{C\text{-}F}$, J = 280.0 Hz), 121.35 (t, CH, J = 3.5 Hz), 125.17 and 127.82 ($d_{C\text{-}F}$, J = 265.0 Hz), 129.10 and 129.13 (d, 2CH, J = 3.5 Hz), 130.34–131.32 ($q_{C\text{-}CF3}$, J = 3.3 Hz), 132.28 (CH), 133.08 (CH), 142.80 (C), 160.43 (C), 168.14 (-N = CH). MALDI-TOF/MS: 348.0657 ($[M + 1]^+$).

2.1.2. 1-[E-({[3,5-bis(trifluoromethyl)phenyl]methyl}imino)methyl] naphthalen-2-ol (Bis-Napht)

FT-IR (υ_{max}, cm^{-1}): 3046.35 (*ar*-H), 1629.71 (C═N), 1277.68 (C—O). ^{1}H NMR (400 MHz, DMSO-d_6, δ ppm): 5.03 (d, 2H, J = 4.0 Hz, CH_2), 6.78 (d, 1H, J = 8.0 Hz, arH), 7.20–7.24 (m, 1H, arH), 7.43–7.48 (m, 1H, arH), 7.65 (dd, 1H, $J_1 = 0.8$, $J_2 = 0.8$ Hz, arH), 7.75 (d, 1H, J = 8.0 Hz, arH), 8.02 (s, 1H, arH), 8.14 (d, 1H, J = 8.0 Hz, arH), 8.17 (s, 2H, arH), 9.38 (d, 1H, J = 8.0 Hz, CH), 11.23 (s, 1H, OH). APT (^{13}C NMR) (100 MHz, DMSO-d_6): 55.32 (CH_2), 107.05 (C), 119.42 (CH), 119.65 and 122.36 ($d_{C\text{-}F}$, J = 271.0 Hz), 121.75 (t, CH, J = 3.5 Hz), 123.04 (CH), 124.60 (CH), 125.08 and 127.79 ($d_{C\text{-}F}$, J = 271.0 Hz), 126.18 (C), 128.34 (2CH), 129.33 (2CH), 130.42–131.40 ($q_{C\text{-}CF3}$, J = 3.3 Hz), 134.33 (C), 137.34 (CH), 142.15 (C), 161.17 (-N = CH), 179.91 (C). MALDI-TOF/MS: 398.164 ($[M + 1]^+$).

2.2. Synthesis of metal complexes

$CuCl_2{\cdot}H_2O$ (1 mmol) in methanol was added dropwise to corresponding ligand (2 mmol) in methanol, and the resultant mixture was stirred at room temperature for 1.5 h. The obtained corresponding solid compound after keeping overnight was filtered and washed with cold methanol, and then dried in air. The FT-IR and MS spectra of the complexes are given in Figs. S9–S12.

Bis-Sal-Cu

FT-IR (υ_{max}, cm^{-1}): 3092.40 (*ar*-H), 1610.12 (C═N), 1283.07 (C—O), 578.70 (M—O), 463.91 (M—N). MALDI-TOF/MS: 817.953 ($[M + 2 + Na]^+$).

Bis-Napht-Cu

FT-IR (υ_{max}, cm^{-1}): 3076.20 (*ar*-H), 1618.78 (C═N), 1279.32 (C—O), 565.46 (M—O), 497.25 (M—N). MALDI-TOF/MS: 917.933 ($[M + 2 + Na]^+$).

2.3. Cell culture growing and cytotoxicity assay

Mouse fibroblast cell (L929), Human cervical cancer cell (HeLa), Human breast adenocarcinoma cell (MCF7) lines were used. Used as a healthy cell line in the study, L929 is generally used for control purposes in studies. Dulbecco's modified Eagle's medium (DMEM), Fetal bovine serum and trypsin–EDTA were supplied from Gibco (Invitrogen). L-glutamine– penicillin–streptomycin solution was from Sigma–Aldrich. The cell lines were maintained in DMEM (Invitrogen) supplemented with 10% FBS, 2 mM L-glutamine, 100U/mL penicillin, and 100 μg/mL streptomycin and kept in a humidified atmosphere at 37°C incubator with 5% CO_2 in air. To determine the effects on cell viability of the compounds Bis-Sal, Bis-Sal-Cu, Bis-Napht, and Bis-Napht-Cu, cells were plated on to 96-well plates (1×10^4 cells/well) for 24 h. The morphology of the cells after the applied dose was examined on the device at 20×

magnification (ZEISS Axio). The in vitro cytotoxicity of the extract was evaluated in the colorimetric 3-(4,5-dimethylthiazolyl-2)-2,5-diphenyltetrazolium bromide (MTT) assay. The MTT assay is used to measure cellular metabolic activity as an indicator of cell viability, proliferation and cytotoxicity. This colorimetric assay is based on the reduction of a yellow tetrazolium salt (MTT) to purple formazan crystals by metabolically active cells. The different concentrations of all compounds (0.1, 1, 10, and 100 μM) prepared in 1% DMSO-growth medium was added on to the cell culture in 96 well plate during 24 h. Each dilution concentration was performed in triplicate. After 24 h, 10 μL of 12 mM MTT (Vybrant, Invitrogen) solution were added into wells and incubated inside a 5% CO_2 store at 37 °C for 4 h. In order to determine the cytotoxic activity of the cells, the absorbance of violet color occurred at the end of 4th hour was measured at 570 nm in a microplate reader (Epoch, USA). As a result of MTT experiments, IC50 values were calculated using Graphpad program and then graphics were created. The selectivity index (SI) of compounds was calculated by obtaining the ratio of IC50 in the healthy cell line/IC50 in the cancer line [24].

2.4. Antimicrobial activity assay

Antimicrobial activity values were determined by the minimum inhibition concentration (MIC) of compounds against microorganisms with the "Microdilution Broth Method" [25]. Microorganism strains used in the study; *Staphylococcus aureus, Pseudomonas aeruginosa, Escherichia coli, Candida albicans*. Mueller Hinton Broth (Accumix® AM1072) for bacterial strains, Saboraud Dextrose Broth (Himedia ME033) for *Candida albicans* was used. The wells on the 11th row were used as sterile control and the wells on the 12th row were used as propagation control. Microorganisms propagated in blood agar broth medium were taken with a loop and a suspension was prepared with these microorganisms at McFarland 0.5 turbidity. Each well was supplemented with 50 μL bacterial suspension as to have 5×10^5 CFU/mL for bacteria and 0.5–2.5 $\times$ 10^3 CFU/mL for *Candida albicans*. Bacteria-supplemented plates were incubated at 37 °C and *C. albicans*- supplemented plates were incubated at 35 °C for 16–24 h. Herein, the first wells in which the appearance of the bacterial colony decreased was accepted as the MIC value. The test was repeated 3 times and the same results were obtained.

2.5. Antioxidant activity assay

To determine of changes in the total antioxidant- oxidant load of the cell lines after administration of the compounds with 10 μM, cells were plated on to 24-well plates (1x10^4 cells/well) for 24 h. After applying 10 μM compound to the cell cultures for 24 h, cell pellet was obtained and homogenization was performed. Homogenates were centrifuged at 3000 rpm for 15 min after homogenization. Supernatants obtained from centrifugation were used for biochemical analyses [26]. After the homogenate was filtered, the manufacturer's protocol was followed in accordance with the procedure of TAS/ TOS kits. Total antioxidant levels (TAS), total oxidant levels (TOS) and oxidative stress index (OSI) values were determined by triplicate experiments with the aid of commercially available Rel Assay Diagnostic kits [27,28]. Trolox standard was used for TAS analyses, hydrogen peroxide standard was used for TOS analyses. Oxidative stress index (OSI) was calculated with the aid of the following equation:

$$\mathrm{OSI\,(AU)} = \frac{\mathrm{TOS,\ \mu mol}\, H_2O_2\ \mathrm{equiv/L}}{\mathrm{TAS,\ mmol\ Trolox\ equiv./L\ X\ 10}}$$

2.6. The assay of interaction with pBR322 plasmid DNA

The interaction of the compounds Bis-Sal, Bis-Sal-Cu, Bis-Napht, and Bis-Napht-Cu with pBR322 plasmid DNA was studied by agarose gel (% 1.5) electrophoresis according to the protocol modified by Bogatarkan et al. [29]. The 40 μL aliquots of increasing concentrations of the complexes, ranging from 1.0 to 100 μM, were added to 1 μL of plasmid DNA (concentration of 0.5 μg/mL) in a buffer solution containing TE buffer (pH = 7.4). The samples were incubated at 37 °C for 24 h in the dark, and then 10 μL aliquots of drug-DNA mixtures were mixed with loading buffer and loaded into 1.5% agarose gel with ethidium bromide. Electrophoresis was carried out under TBE buffer (pH = 8.0) for 5 h at 40 V. The gel was then viewed with a UV transilluminator and the image was captured as a photograph (Syngene).

2.7. Statistical analysis

SPSS 23.0 (IBM Corparation, Armonk, New York, United States) program was used for statistical data analysis. The data were analyzed at 95% confidence level, and if the p value was <0.05, it was considered significant. Results are given as mean ± SD. The statistical significance levels of the doses are given on the figures ($*p < 0.05$, $**p < 0.01$ and $***p < 0.001$).

2.8. Theoretical calculations

Theoretical calculations provide important information about the chemical and biological properties of compounds. Many quantum chemical parameters are obtained from theoretical calculations. The calculated parameters are used to explain the chemical activities of the compounds. Many programs are used to calculate compounds. These programs are Gaussian09 RevD.01 and GaussView 6.0 [30,31]. By using these programs, calculations were made in B3LYP, HF, and M06-2x [18–20] methods with the 6–31++g(d,p) basis set. As a result of these calculations, many quantum chemical parameters have been found. Each parameter describes a different chemical property of compounds, the calculated parameters are calculated as follows. [32,33].

$$\chi = -\left(\frac{\partial \mathrm{E}}{\partial \mathrm{N}}\right)_{\upsilon(r)} = \frac{1}{2}(I+A) \cong -\frac{1}{2}(E_{HOMO}+E_{LUMO})$$

$$\eta = -\left(\frac{\partial^2 \mathrm{E}}{\partial \mathrm{N}^2}\right)_{\upsilon(r)} = \frac{1}{2}(I-A) \cong -\frac{1}{2}(E_{HOMO}-E_{LUMO})$$

$$\sigma = 1/\eta\omega = \chi^2/2\eta\varepsilon = 1/\omega$$

A technique exists for contrasting the biological actions of the ligand and its metal complexes with those of enzymes. Molecular docking is the most typical of them. Metal complexes can be compared using a few of these molecular docking techniques. The HEX software is employed in this investigation. These enzyme proteins interact with the ligand and its metal complexes to boost their biological activity [34]. Compounds' biological activities were compared to those of enzymes using molecular docking calculations. Using the optimized compound's structure and the Gaussian software, a file with the.pdb extension was produced [31]. At HEX 8.0.0, the enzyme and compound files were examined [35]. For docking, the following variables are used: Correlation typeshape only, 3D FFT mode, 0.6-dimensional grid, 180-degree receptor and ligand ranges, 360-degree twist range, and 40-degree distance range. The interaction between the chemicals and the proteins was also thoroughly examined using the Protein-Ligand Interaction Profiler (PLIP) service [36,37]. The interaction between the chemicals and the proteins was also thoroughly examined using the Protein-Ligand Interaction Profiler (PLIP) service.

3. Results and discussion

3.1. Synthesis

The two novel Schiff base ligands were synthesized by condensation of salicylaldehyde and 2-hydroxy-1-naphthaldehyde with 3,5-bis

Table 1
Analytical and physical data for ligands and their metal complexes.

Comp.	Molecular Formula (g/mol)	Color	Yield (%)	Λ_m*	μ_{eff} (BM)	Found (calcd.) %		
						C	H	N
Bis-Sal	$C_{16}H_{11}F_6NO$, 347.26	Yellow	89	–	–	55.13 (55.34)	3.36 (3.19)	4.21 (4.03)
Bis-Napht	$C_{20}H_{13}F_6NO$, 397.31	Light Yellow	84	–	–	60.64 (60.46)	3.19 (3.30)	3.43 (3.53)
Bis-Sal-Cu	$C_{32}H_{24}F_{12}N_2O4Cu$, 792.070	Olive	77	23.54	1.89	48.26 (48.52)	3.15 (3.05)	3.38 (3.54)
Bis-Napht-Cu	$C_{40}H_{28}F_{12}N_2O_4Cu$, 892.188	Dark Yellow	81	24.01	1.91	53.63 (53.85)	3.02 (3.16)	3.10 (3.14)

*(Ohm^{-1} cm^2 mol^{-1}).

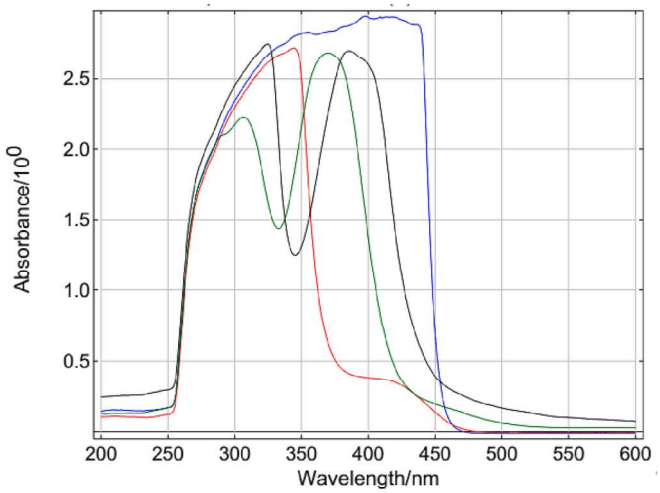

Fig. 1. Electronic spectra of ligands and their Cu(II) complexes.

(trifluoromethyl)benzylamine following by previously reported method [2,5]. The copper(II) complexes was prepared by the reaction of obtained ligands with $CuCl_2{\cdot}2H_2O$ in methanol, according to early described procedure [2,4] (Scheme 1). The ligands and their metal complexes were found to be stable in air at room temperature, and are soluble in most common organic solvents such as CH_2Cl_2, $CHCl_3$, acetone, DMSO, DMF. The physical and analytical data for all synthesized compounds were summarized in Table 1. The reaction of **Bis-Sal** and **Bis-Napht** with $CuCl_2{\cdot}2H_2O$ in 1:2 ratio (M:L) leads to the formation of 1:2 ($M:L_2$) complexes.

The spectral and analytical data of the obtained compounds were consistent with their proposed structures. Many attempts were made to crystallize complex compounds, such as different solvent systems, soaking in solvent at room temperature, evaporation under reduced pressure, but unfortunately, the crystal structure could not be achieved as a result of the trials.

3.2. Spectroscopic analysis

3.2.1. Molar conductivity

The molar conductivity measurements were performed at room temperature in 5×10^{-4} M concentration using DMF as solvent. The ligands were not electrically conductive, while the corresponding copper complexes were found to be non-electrolytic in nature with low values of 23.54 Ohm^{-1} cm^2 mol^{-1} (for Bis-Sal-Cu) and 24.01 Ohm^{-1} cm^2 mol^{-1} (for Bis-Napht-Cu) [38].

3.2.2. Electronic spectra and magnetic behavior

The UV–Vis spectra of the ligands and their Cu(II) complexes in DMSO are shown in Fig. 1. The UV–Visible spectra of the synthesized ligands and their Cu(II) complexes allow for the first explanation to be deduced that the electronic transitions of the complexes shift smoothly compared to their corresponding ligands. These shifting can be attributed to the rigidity from the two aromatic units after the coordination reaction, and therefore the energy required for electron transition from the ground state to the excited state is decreased. Eventually, the absorption of the Schiff base ligands are red shifted after coordination with Cu(II) ion.

The $\pi \rightarrow \pi^*$ transition of the compound Bis-Sal was observed around 341 nm, while the $\pi \rightarrow \pi^*$ transition of the compound Bis-Napht occurred at 355 nm in UV–Vis. Likewise, the $n \rightarrow \pi^*$ transitions of the ligands appeared around 412 nm and 415 nm which originated from azomethine (C═N) chromophore group, respectively. The novel bands occured higher wavelenght in the UV–Vis spectra of the synthesized Cu(II) complexes could be attributed to the ligand–metal charge transfer band (LMCT) confirming the coordination of its nitrogen and oxygen atoms to the metallic ions. The compound Bis-Sal-Cu exhibited three bands which are 306 nm, 370 nm and 518 nm, while the novel bands of the compound Bis-Napht-Cu appeared at 322 nm, 387 nm, and 524 nm. Further, the magnetic moment values of Bis-Sal-Cu and Bis-Napht-Cu, determined as 1.89 BM and 1.91 BM, were found within the suggested range for octahedral geometry.

3.2.3. FTIR analysis

The FT-IR spectra of the ligands and their Cu(II) complexes were recorded in the range of 400–4000 cm^{-1} to demonsrate the presence and changing of functional groups. The disappearance and shifting of position and intensities of some spectral peaks were predicted to happen during the complexation process. The sharp bands observed at 1633.61 cm^{-1} and 1629.71 cm^{-1} for the ligands Bis-Sal and Bis-Napht, respectively attributed to azomethine group (-C═N-). These bands in the corresponding Cu(II) complexes were detected at lower wavenumber, with values of 1610.12 cm^{-1} for Bis-Sal-Cu and 1618.78 cm-1 for Bis-Napht-Cu due to the donation of lone pair of electrons of nitrogen atom to copper ion [39,40].

The presence of strong bands in the range of 1115.58 and 1167.73 cm^{-1} assigned to υ(—CF_3) stretching vibrations, proved the presence of CF_3 bond in all obtained compounds [41]. The phenolic hydroxyl bands are generally found at about 3500 cm-1, but υ(–OH) weak bands were not seen in FT-IR spectra of our ligands since it could be the formation of intramolecular hydrogen bond. However, the high intensity band at 1278.56 cm^{-1} for the compound Bis-Sal and 1277.68 cm^{-1} for the compound Bis-Napht related to phenolic C—O linkage were found higher wavenumbers for the corresponding Cu(II) complexes. These results suggest that the absence of hydrogen of hydroxyl group and the shifting C—O bands proved the involvement of deprotonated phenolic groups in bond formation with the copper atom. Moreover, the presence of new bands in the spectra of these complexes occured between 578.70 and 565.46 cm^{-1} and 463.91–497.25 cm^{-1} are assigned to M—O and M—N vibration bands, respectively [42]. The FT-IR spectra of ligands and Cu(II) complexes are given in supplementary file.

3.2.4. NMR analyses

The ^1H NMR signals attributed to phenolic hydroxyl group in the compounds Bis-Sal and Bis-Napht were resonated at 13.02 ppm and 13.20 ppm, respectively. The aromatic –CH proton peaks were observed in the range of 6.78 ppm and 8.17 ppm. Further, the $–CH_2$ protons were resonated at 4.96 ppm for compound Bis-Sal and 5.03 ppm for compound Bis-Napht. The formation of the azomethine (N = CH) proton is

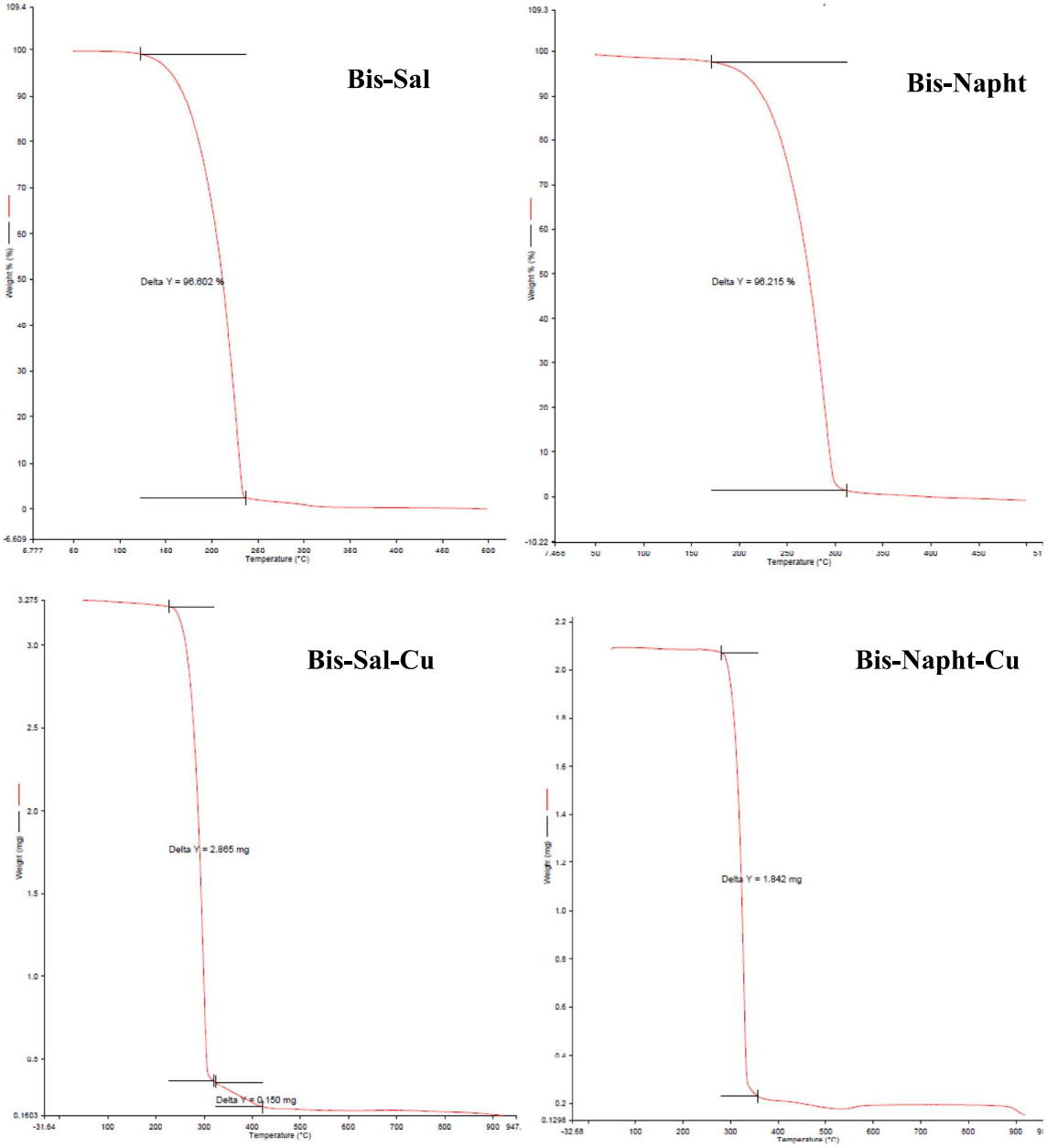

Fig. 2. TGA analysis curve of ligands and Cu(II) complexes.

the most important proof in Schiff base synthesis [43]. This proton in the structure of the synthesized ligands was resonated 8.75 ppm (compound Bis-Sal) and 9.38 ppm (compound Bis-Napht) and supports the formation of the structures. Besides, in ^{13}C NMR (APT) of the synthesized ligands, the aromatic carbon signals were demonstrated in the region of 107.05–179.91 ppm. The peaks at 160.43 ppm and 161.17 ppm, respectively, proving the presence of the azomethine carbon atom in the ligands supported the formation of the proposed structures. The carbon peaks of CH_2 linked to phenyl ring and azomethine group were observed at 61.23 ppm (for Bis-Sal) and 55.32 pp (for Bis-Napht). Additionally, the carbon atoms of CF_3 groups for both compounds were resonated as doublet in the region of 119.65–127.82 ppm. The aromatic carbons linked to CF_3 groups were found as quartet for Bis-Sal (130.83 ppm) and Bis-Napht (130.91 ppm).

3.3. TGA analysis

The thermal stability of ligands and their Cu(II) complexes were performed by a PerkinElmer TGA-8000 thermogravimetric analyzer. Samples were heated (50–500 °C for ligands and 50–1000 °C for complexes) at a rate of 10 °C/min under an N_2(g) with a flow rate of 20 mL/min. It was observed that the compound Bis-Sal was thermally stable up to 120 °C, coinciding with its melting point in the TGA curve, and decomposition occurred with a material loss of 96.6% between 122 °C and 241 °C. Likewise, the decomposition took place in the range of 171 °C and 316 °C with a loss of 96.2%, while the compound Bis-Napht was thermally stable up to 170 °C. The copper complexes displayed higher thermal stability than the corresponding ligands. The TGA curve of the compound Bis-Sal-Cu was found to be stable up to 233 °C, then the decomposition started from 234 °C to 319 °C with loss of 88%, and a second curve was observed in the range of 320 °C and 422 °C resulting in a mass loss of 4.6%. The compound Bis-Napht-Cu was completed by a

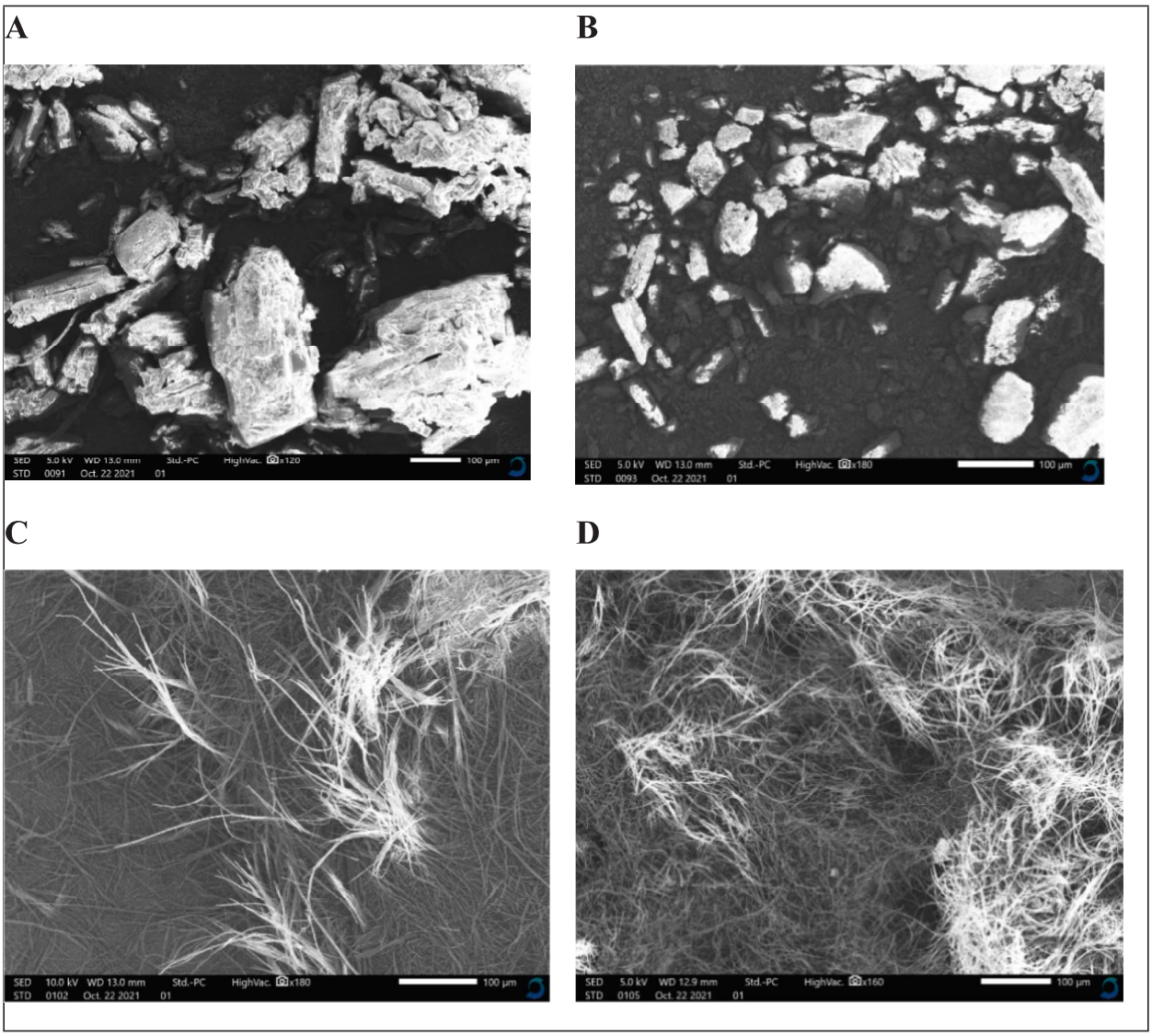

Fig. 3. SEM images of the synthesized compounds.

Table 2
Comparison of IC50 values of the synthesized compounds in cell lines.

IC50 (μM ± SD)			
Compounds	**HELA cell line**	**MCF-7 cell line**	**L929 cell line**
Bis-Sal	35 ± 1 μM	36 ± 1 μM	106 ± 9 μM
Bis-Napht	3 ± 1 μM	5 ± 1 μM	3 ± 1 μM
Bis-Sal-Cu	16 ± 2 μM	17 ± 2 μM	13 ± 5 μM
Bis-Napht-Cu	2 ± 1 μM	16 ± 1 μM	16 ± 6 μM
Cisplatin	26 ± 2 μM	32 ± 3 μM	229 ± 5 μM

total decomposition in the temperature between 280 and 358 °C, with 88 % weight loss. The amount of mass remaining without decomposition can be interpreted as the residues of the metal ion present in the complexes in Fig. 2.

3.4. SEM analysis

The SEM analysis were performed using a JEOL JCM-7000 Neoscope™. The scanning electron micrographs revealed the morphology of the Schiff bases and their Cu(II) complexes (Fig. 3A–D). The SEM micrograph of the Bis-Sal and Bis-Napht exhibited irregular broken rock shape morphology where the particles of about micrometer size were also randomly distributed over these rock shape structures. Moreover, according to the surface morphology of the complexes demonstrated threadlike images.

3.5. Cytotoxic activity results

In present study, cytotoxic activities of the compounds Bis-Sal, Bis-Sal-Cu, Bis-Napht, and Bis-Napht-Cu were evaluated in Table 2 and Fig. 4. The percentages of survival of cells after administration of the compounds were calculated and compared with each other. IC_{50} doses of compounds applied to cells were found to be more effective in MCF 7 cells. The compound Bis-Napht showed the highest cytotoxic activity with an IC50 dose of 5 ± 1 μM amongst the compounds performed to MCF 7 cells. The compound Bis-Napht-Cu exhibited the highest cytotoxic activity with an IC50 dose of 2 ± 1 μM on HeLa cells. All compounds, except for the compound Bis-Sal, demonstrated cytotoxic activity on L929 cell line. It was determined to have lower cytotoxic activity in L-929 cells at an IC50 dose of 106 ± 9 μM at 24 h compared to other compounds. Further, it was clear that the compound Bis-Napht showed the highest cytotoxic activity with IC50 dose that very lower than 10 μM on both three cell lines. The other compounds were

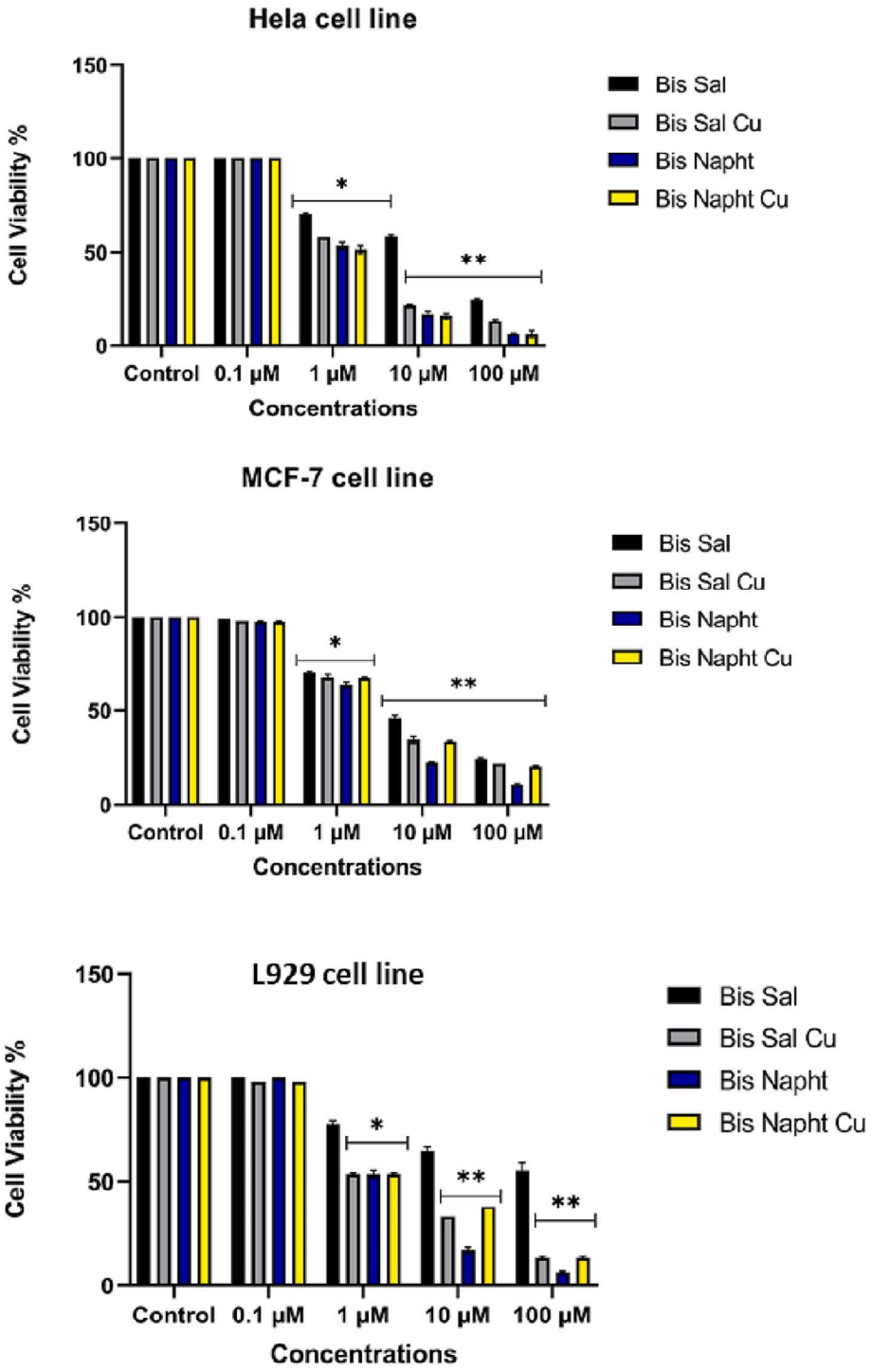

Fig. 4. Determination of the cytotoxic activity of compounds in MCF-7, HeLa and L929 cell lines. Activities of compounds after 24-hour incubation at concentrations ranging from 0.1 to 100 µM (* $P < 0.05$; **$P < 0.01$).

Table 3
The selectivity index (SI) of compounds at 24 h treatment.

Compound	L929/MCF 7	L929/HeLa
Bis-Sal	3.0 ± 0.7	3.0 ± 0.8
Bis-Napht	0.6 ± 0.1	1.0 ± 0.1
Bis-Sal-Cu	0.8 ± 0.2	0.8 ± 0.3
Bis-Napht-Cu	1.0 ± 0.8	8.0 ± 1.1
Cis-platin	7.0 ± 1.3	8.2 ± 1.5

generally found to be higher than 10 µM on cell lines in Table 2. In some studies in the literature, copper ions from salt solutions or metal complexes have been shown to be toxic in some in vitro cell culture studies [43–45]. However, according to the results of the study, in the case of copper, cytotoxicity is also related to the local concentration of the released ions and the exposure time. In addition, local biological effects of ions, when pure metals or alloys are used as biomaterials in the body, their synergistic and antagonistic effects and interactions between externally added copper ions and ions and molecules in the cell have not been fully explained. Therefore, it would be a different study to show the

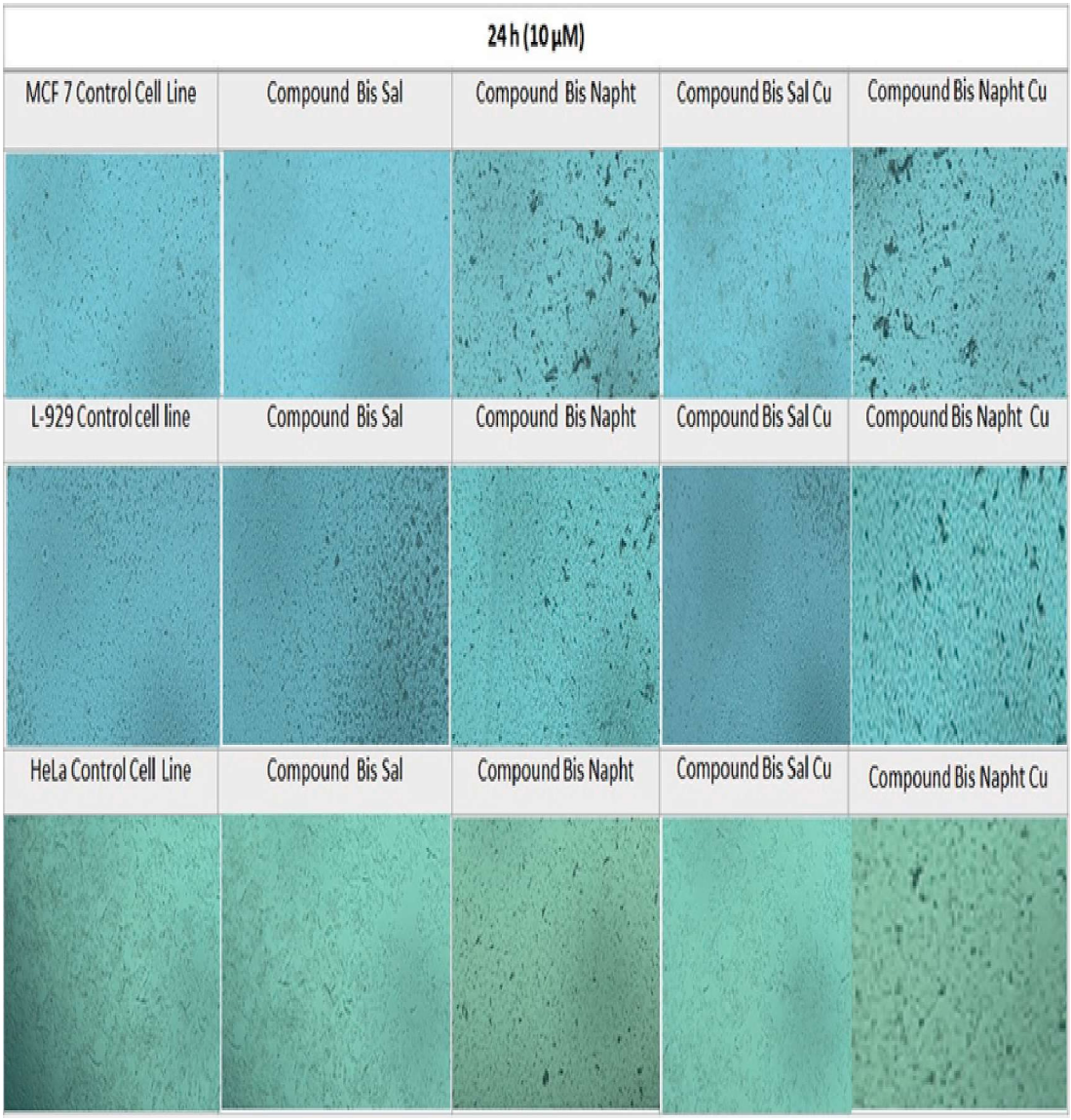

Fig. 5. Morphological changes of cells after 24 h of incubation with 10 μM dose of all compounds.

Table 4
MIC values on some microbial strains of the synthesized compounds.

	MIC values (mg mL^{-1})			
Compound	*E. coli*	*S. aureus*	*P. aeroginosa*	*C. albicans*
Bis-Sal	>5	>5	>5	>5
Bis-Napht	0.63	1.35	1.35	0.63
Bis-Sal-Cu	0.31	0.31	0.63	0.63
Bis-Napht-Cu	0.31	0.16	0.31	0.15

effect of copper ions used in the newly synthesized compounds used in the study in cells, and it was never mentioned in this study.

As a matter of fact, it is accepted by the NCBI cancer institute that compounds with IC50 values above 10 μM do not have a significant anticarcinogenic effect. So advanced anticancer analyses were not conducted since IC50 values of compounds on cell lines were higher than 10 μM threshold. However, by using IC50 values, it is possible to compare the compounds on 3 cell lines to determine to provide which cell lines are more affected by using Selectivity Index (SI) (Table 3). The SI value of the compound Bis-Napht-Cu was the highest. These results suggest that the compound Bis-Napht-Cu is more cytotoxic towards

Table 5
TAS, TOS and OSI values from MCF-7, HeLa and L929 cell lines that are treated with all compounds during 24 h (Values are presented as mean ± SE; Experiments were made in triplicate).

Mean ± S.E.		MCF-7	HeLa	L929
TAS values	Control	0.41 ± 0,01	0.50 ± 0.01	0.40 ± 0.01
	Bis-Sal	0.40 ± 0,01	0.50 ± 0.01	0.40 ± 0.01
	Bis-Napht	0.38 ± 0,01	0.48 ± 0.02	0.38 ± 0.01
	Bis-Sal-Cu	0.36 ± 0,02	0.45 ± 0.02	0.36 ± 0.01
	Bis-Napht-Cu	0.33 ± 0,01[a]	0.45 ± 0.02	0.34 ± 0.02
TOS values	Control	0.74 ± 0.03	0.84 ± 0.04	0.71 ± 0.03
	Bis-Sal	0.73 ± 0.02	0.80 ± 0.04	0.72 ± 0.02
	Bis-Napht	0.75 ± 0.03	0.84 ± 0.05	0.71 ± 0.03
	Bis-Sal-Cu	0.78 ± 0.03	0.86 ± 0.06	0.74 ± 0.05
	Bis-Napht-Cu	0.78 ± 0.04	0.89 ± 0.05[e]	0.76 ± 0.06[f]
OSI values	Control	0.22 ± 0.01	0.17 ± 0.01	0.18 ± 0.01
	Bis-Sal	0.18 ± 0.	0.16 ± 0.01	0.18 ± 0.01
	Bis-Napht	0.20 ± 0.01	0.18 ± 0.01	0.19 ± 0.01
	Bis-Sal-Cu	0.22 ± 0.01	0.19 ± 0.01	0.21 ± 0.01
	Bis-Napht-Cu	0.24 ± 0.01 [g]	0.20 ± 0.01 [h]	0.22 ± 0.01 [k]

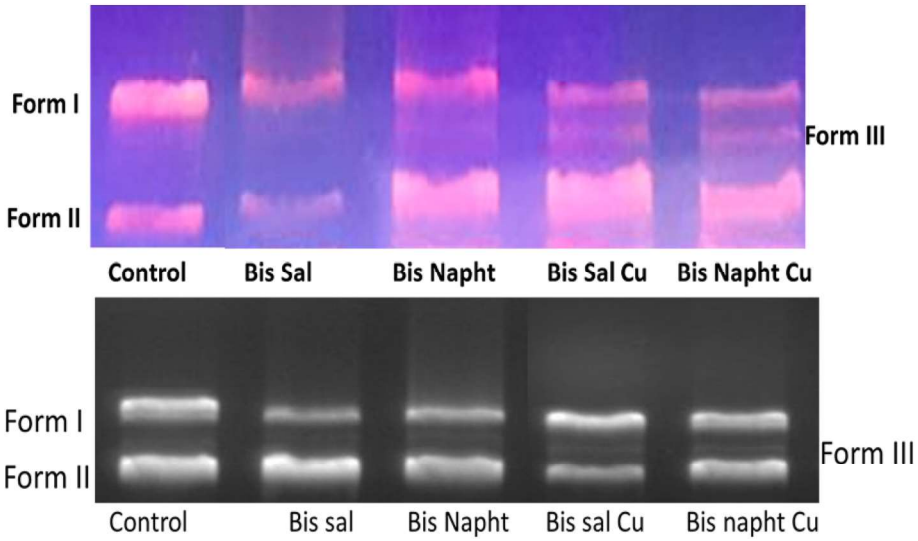

Fig. 6. Visualization of gel electrophoretic pattern of pBR322 plasmid DNA when incubated with 100 μM concentrations of all compounds. The colourful image is a direct agarose gel electrophoresis image, and the black cloured image is taken from the gel imaging system (SynGene).

Table 6
The calculated quantum chemical parameters of compounds.

	E_{HOMO}	E_{LUMO}	I	A	ΔE	η	μ	χ	Pİ	ω	ε	dipol	Energy
B3LYP/6–31 g LEVEL													
1	−6.6666	−2.4153	6.6666	2.4153	4.2513	2.1256	0.4704	4.5409	−4.5409	4.8503	0.2062	5.0712	−37042.4458
2	−5.9675	−2.2602	5.9675	2.2602	3.7073	1.8537	0.5395	4.1138	−4.1138	4.5650	0.2191	4.2516	−117818.8187
3	−6.1678	−2.3761	6.1678	2.3761	3.7917	1.8958	0.5275	4.2719	−4.2719	4.8131	0.2078	5.1326	−41222.1873
4	−5.9814	−2.3152	5.9814	2.3152	3.6662	1.8331	0.5455	4.1483	−4.1483	4.6937	0.2131	5.3301	−126178.9933
HF/6–31 g LEVEL													
1	−8.8693	0.9192	8.8693	−0.9192	9.7886	4.8943	0.2043	3.9751	−3.9751	1.6143	0.6195	4.7386	−36847.0315
2	−5.7490	0.6025	5.7490	−0.6025	6.3515	3.1757	0.3149	2.5733	−2.5733	1.0425	0.9592	4.9500	−117386.3615
3	−8.0291	0.9247	8.0291	−0.9247	8.9537	4.4769	0.2234	3.5522	−3.5522	1.4093	0.7096	4.2694	−40999.6618
4	−7.5763	0.6291	7.5763	−0.6291	8.2054	4.1027	0.2437	3.4736	−3.4736	1.4705	0.6801	4.8927	−125694.9447
M062X/6–31 g LEVEL													
1	−7.9866	−1.2621	7.9866	1.2621	6.7245	3.3623	0.2974	4.6243	−4.6243	3.1801	0.3145	4.9288	−37028.4866
2	−7.0851	−1.3924	7.0851	1.3924	5.6927	2.8463	0.3513	4.2388	−4.2388	3.1562	0.3168	6.0896	−117789.1749
3	−7.3811	−1.2305	7.3811	1.2305	6.1506	3.0753	0.3252	4.3058	−4.3058	3.0143	0.3317	4.6253	−41206.5560
4	−7.1047	−1.4507	7.1047	1.4507	5.6540	2.8270	0.3537	4.2777	−4.2777	3.2363	0.3090	4.3307	−126145.9609

HELA cancer cell lines and is more selective than other compounds. Besides, the compound Bis-Napht-Cu exhibited moderate selectivity index on the MCF7 cell line. The compound Bis-Sal showed almost the same selectivity index values on both MCF-7 and HeLa cells in Table 3. In this study, we used cisplatin as a positive control in MTT experiments. Although cisplatin is not similar in structure to the synthesized compounds, we have included it in the Tables 2 and 3. Cisplatin, which is effective in low concentration, is a highly effective drug in chemotherapy. It is seen that cisplatin is used as a positive control in our previous studies on this subject [46].

Morphological analyzes were performed 24 h after the administration of all synthesized compounds at a dose of 10 μM to three cell lines in Fig. 5. It was found that the compound Bis-Napht- Cu was found to significantly alter the morphology in HeLa cell line. Also the compound Bis-Napht was found to significantly alter the morphology in all the cell lines compared to the control group in Fig. 5. In morphological analyses, the compounds were placed in the medium at a concentration of 10 μM, cell separation and structural integrity were evaluated. At this point, it was determined that the Bis-Napht-Cu compound was more effective on Hela cells. It seems that the Bis-Napht compound may cause the compounds to weaken intercellular communication in both MCF-7 and HeLa cells. In order to compare whether the effect studied with wide ranges on cell viability shows morphologically on the cell, single-dose control cell images were examined.

3.6. *Antimicrobial activity results*

Antimicrobial activity of the compounds is provided in Table 4. It is reported to be significant when the antimicrobial activity values of the studied materials are 0.1 mg mL^{-1} or less, moderately effective in the range of 0.1 < MIC ≤ 0.625 mg mL^{-1}, and weakly effective when the MIC value is >0.625 mg mL^{-1} [37,47]. The Bis-Sal-Cu and Bis-Napht-Cu compounds have been found to be moderately effective on all microorganisms we have tried in this study. In addition, the compound Bis-Sal did not show any antimicrobial activity in Table 4. However, there are many microorganisms that the antimicrobial activities of these chemicals can be investigated. By looking at their effects on other microorganisms, the antimicrobial effect of these compounds can be revealed more clearly.

3.7. *Oxidant and antioxidant capacities of compounds*

Antioxidant potentials of compounds generally come from their anti-scavenging activity on reactive oxygen species. Antioxidant substances

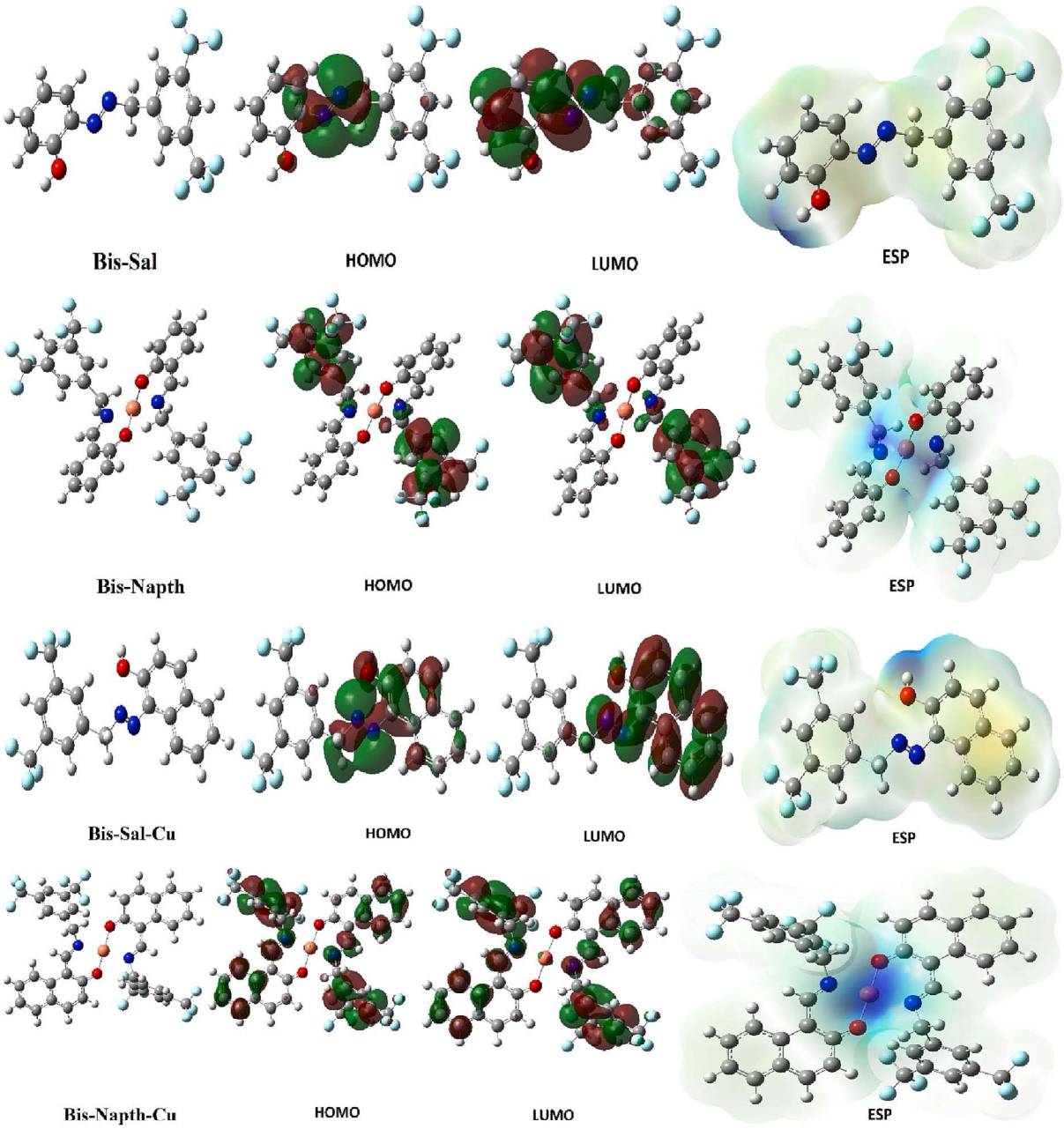

Fig. 7. Representations of optimized structures, HOMO, LUMO, and ESP of compounds.

Table 7
E_{total} energy value for all compound in molecular docking.

	1JNX	4GBH
Bis-Sal	−246.48	−266.86
Bis-Napht	−301.35	−337.58
Bis-Sal-Cu	−269.52	−290.82
Bis-Napht-Cu	−397.73	−370.47

eliminate harmful reactions of free radicals and thus prevent degenerative diseases [26]. TAS values of the cells applied the compounds are found generally low and statistically nonsignificant compared to control group generally ($P > 0.05$). Although the antioxidant capacity of the cell cultures to which the compound BS was applied decreased, it was determined that the differences were insignificant ($P > 0.05$) in Table 5. When the capacity of the test compounds to change the total oxidant levels (TOS) of cell cultures was evaluated, it was observed that the oxidant level increased in general 24 h after the application of the compounds except for the compound Bis-Sal. Also, the increases of TOS are statistically non-significant ($P > 0.05$) except for Bis- Napht-Cu compound in all cell line applications in Table 5. On the other hand, statistically insignificant increases were determined in OSI values from almost all experimental groups compared to control group in Table 5. Oxidative stress index is expressed as the ratio between total oxidant levels and total antioxidant levels. As for groups which increased OSI values significantly compared to values from control group, this can be explained as cellular damage is occurring in the cell metabolism due to increased formation and amounts of lipid peroxidation and reactive oxygen species.

3.8. *Interaction with pBR322 plasmid DNA and compounds*

Nowadays it is accepted that the antineoplastic activity of the drug is based on its interaction with cellular DNA. Because if the cell cannot

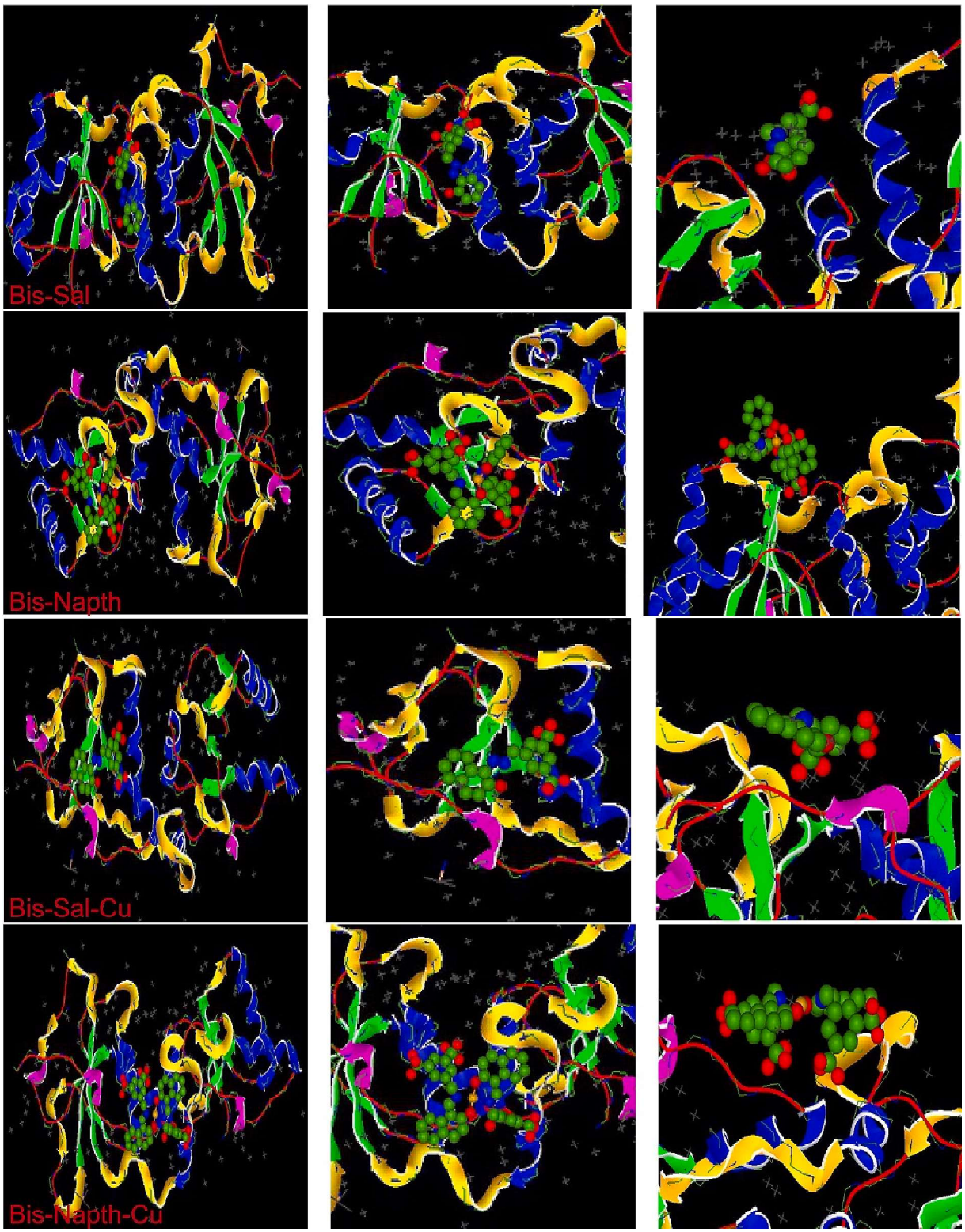

Fig. 8. Presentation interactions of all compounds with breast cancer protein.

remove the DNA damage, by the time the cells die by one of metabolic pathways [29,48]. In this research the effect of the compounds binding on pBR322 plasmid DNA tertiary structure was investigated by their ability to modify the electrophoretic mobility of supercoiling of closed circular pBR322 plasmid DNA by using electrophoresis technique on agarose gels. There are normally 2 forms of pBR322 plasmid DNA. Form I intacs covalently closed circular form and run fast. If modifying occurs on one chain, the supercoiled form will relax to generate a slower-moving open circular form II. If both double chains are cleaved by any factor, linear form III that migrates between form I and form II will be presented. Within the scope of this study, pBR322 plasmid DNA was treated with 4 different doses of compound in the range of 0.1–100 μM at 37 °C for 24 h. No interaction between plasmid DNA bands was detected at other low doses except the 100 μM dose and there were 2 bands as

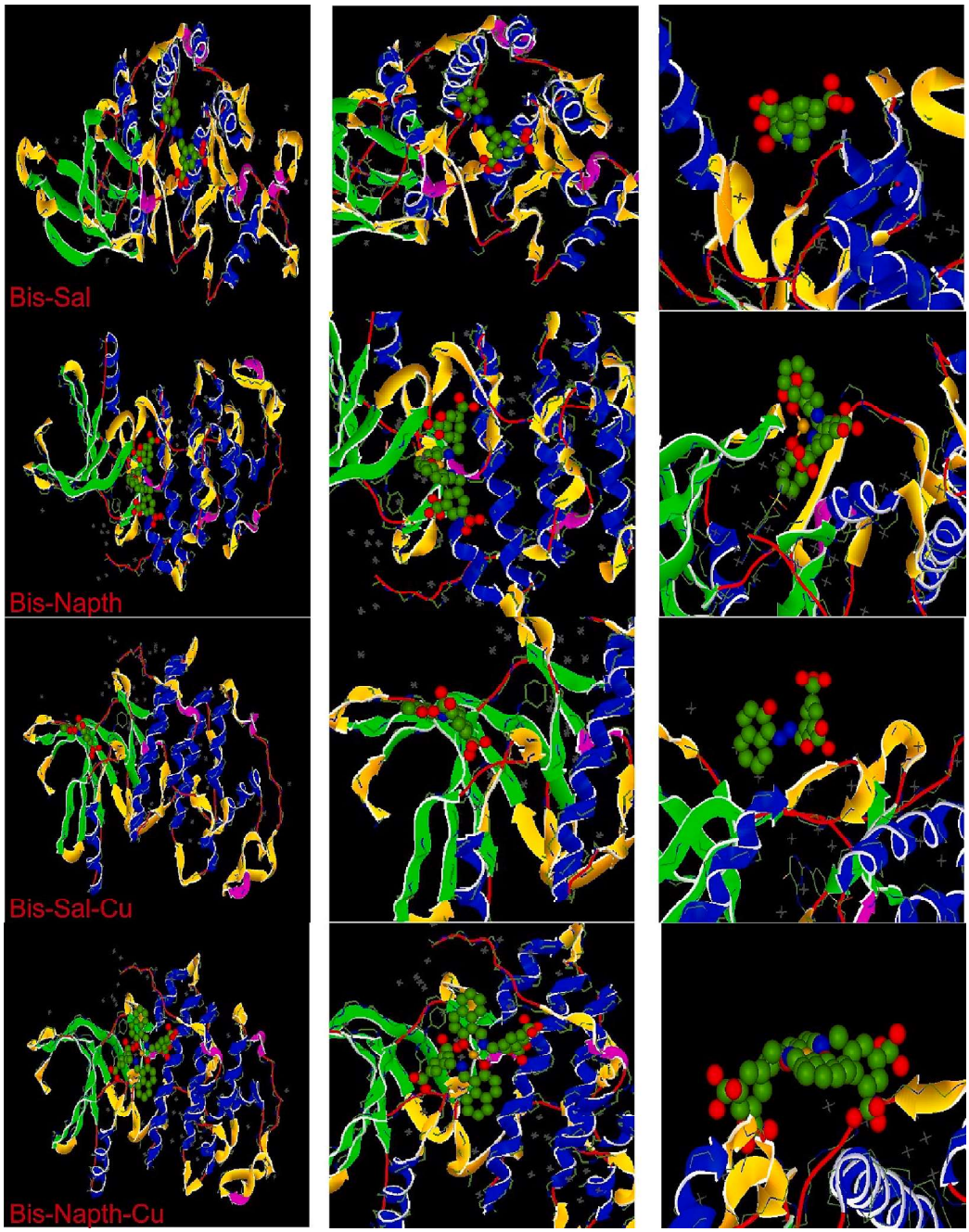

Fig. 9. Presentation interactions of all compounds with cervical cancer protein.

Form I and II on the gel. But after exposure of plasmid DNA with compounds at 100 μM dose for 24 h, the linear third band was appeared. In the visualization of the plasmid DNA incubated with high concentration (100 μM) compounds, it was observed that the form I and form II bands' density decreased, while the form III band appeared between these 2 bands placed on the gel in Fig. 6. This electrophoretic visualization pattern of pBR322 plasmid DNA forms is consistent with previous reports [29,49]. This situation can relate with the unwinding of supercoiled DNA to open circular and linear DNA. Except for the compound Bis-Sal, the other compounds almost the same banding pattern in Fig. 6. All the form I, II and III bands were observed at just 100 μM high concentrations of the compounds Bis-Sal-Cu, Bis-Napht, and Bis-Napht-Cu application on pBR322 plasmid DNA.

3.9. Theoretical calculations

Theoretical calculations are an important method used to predict the activities of compounds quickly and easily. As a result of the first Gaussian calculations, many parameters are calculated. Each calculated parameter provides information about many different properties of compounds. Among these parameters are two parameters that determine the activities of the compounds, which are HOMO and LUMO. These two calculated parameters are widely used to compare the activities of compounds [32]. HOMO parameter of compounds shows the ability of compounds to donate electrons, and the compound with the most positive numerical value of this parameter has the highest activity [50]. On the other hand, the numerical value of the LUMO parameter of the compounds indicates the acceptability of the compounds, which the numerical value of the parameter with the most negative value has the

Table 8
Hydrophobic Interactions of protein and metal complex of compounds.

Index	Residue	AA	Distance	Ligand atom	Protein atom
Breast cancer protein-Bis-Napht-Cu					
1	1742X	ASN	3.90	2030	870
2	1746X	HIS	3.51	2031	898
3	1844X	LEU	3.81	2005	1709
4	1846X	GLN	3.11	1994	1729
5	1848X	GLN	4.00	1991	1743
6	1849X	GLU	3.88	1995	1754
Cervical cancer protein-Bis-Napht-Cu					
1	61A	PRO	3.23	2809	507
2	61A	PRO	2.89	2832	508
3	113A	GLN	3.81	2835	1021
4	291A	LYS	3.49	2788	2612

In table: ASN: Asparagine, HIS: Histidine, LEU: Leucine, GLN: Glutamine, GLU: Glutamate.

higher activity [51]. As a result of the calculations, considering the values of the calculated parameters, it is seen that the compound Bis-Napht has a more positive value than the other compounds according to the numerical value of the HOMO parameter. On the other hand, according to the numerical value of the LUMO parameter of the compounds, it is seen that the Bis-Napht-Cu metal complex at the B3LYP level has higher activity in the others. All parameters obtained from the calculations are given in Table 6.

Moreover, another calculated parameter is the ΔE energy gap parameter, which is known to have high activity if the numerical value of this parameter is low [50]. Another parameter is electronegativity, which shows the ability of compounds to attract electrons, the numerical value of this parameter is known to have the highest activity of the smallest compound [51].

It should be well known that absolute hardness and softness are important properties for measuring molecular stability and reactivity. As said in the study by Kaya et al. [52], the term chemical hardness showed that the electron cloud of atoms, ions or molecules refers to the

Table 9
Hydrogen Bonds of Breast cancer protein-Bis-Napht-Cu.

Index	Residue	AA	Distance H-A	Distance D-A	Donor angel	Protein donor?	Side chain	Donor Atom	Acceptor Atom
Staphylococcus aureus -metal complex									
1	291A	LYS	2.29	3.22	147.83	√	√	2614 [N3 +]	2804 [O2]

In table: LYS: Lysine.

Table 10
Water Bridges of Breast cancer protein-BN-Cu.

Index	Residue	AA	Dist. H-A	Dist. D-A	Donor angle	Water angle	Protein donor?	Donor atom	Acceptor atom	Water atom
1	113A	GLN	3.09	2.98	108.38	90.69	√	1024 [N3]	2844 [O2]	2724

In table: GLN: Glutamine.

Table 11
π-Cation Interactions of Cervical cancer protein-BN-Cu.

Index	Residue	AA	Distance	Offset	Protein charged?	Ligand group	Ligand atoms
1	291A	LYS	3.09	1.27	√	Aromatic	2788, 2789, 2790, 2791, 2793, 2795

In table, LYS: Lysine.

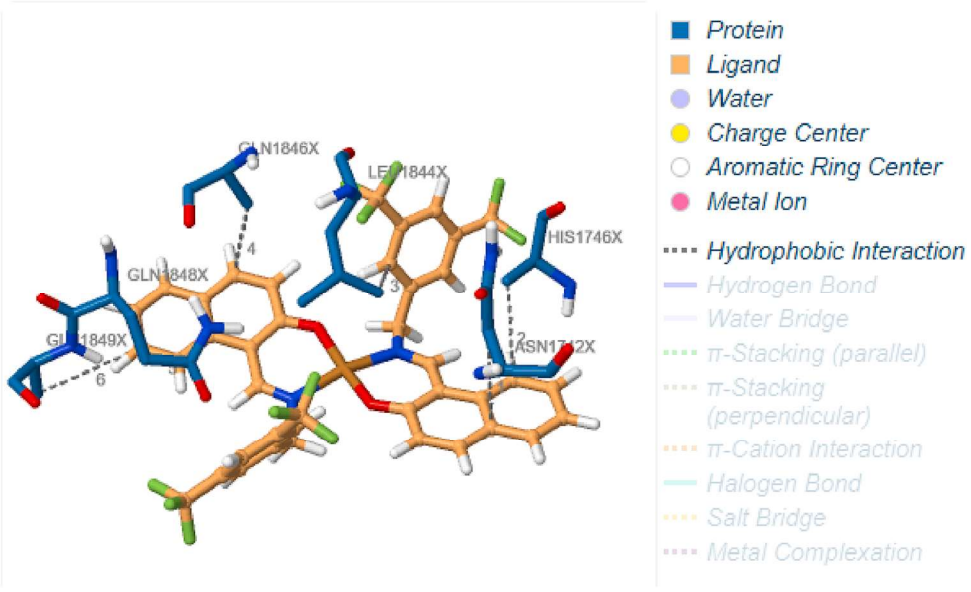

Fig. 10. Presentation interactions of Breast cancer protein with Bis-Napht-Cu.

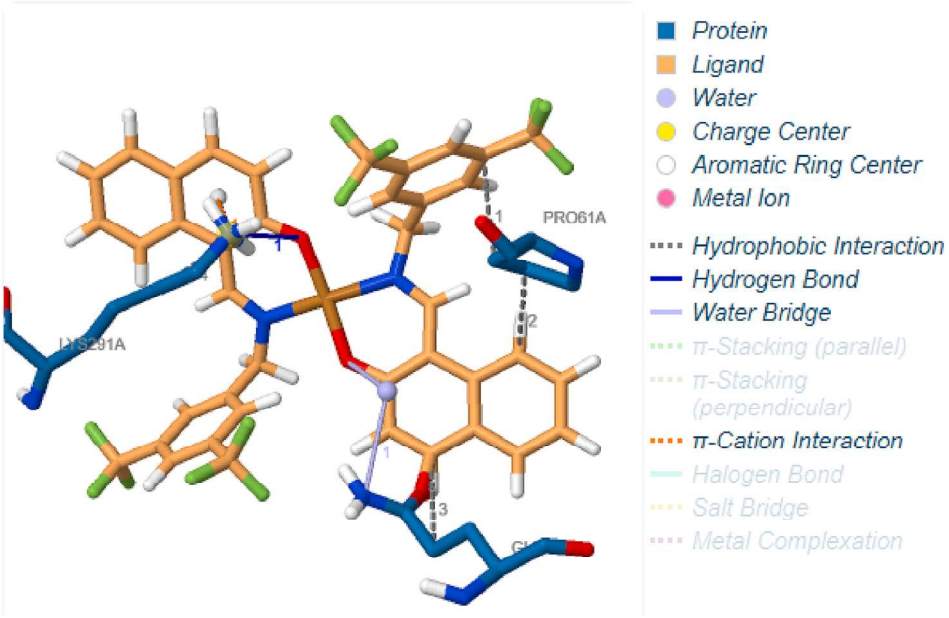

Fig. 11. Presentation interactions of cervical cancer protein with Bis-Napht-Cu.

resistance to deformation or polarization under small perturbation of a chemical reaction. However, a molecule with a hard property has a large energy gap, whereas a molecule with a soft property has a small energy gap.

Therefore, molecules with the lowest values of spherical hardness. It is known to have higher activity than other molecules. It takes place in the part of a molecule that has the greatest softness and lowest hardness. It is known that the molecule with the lowest value of spherical hardness (hence the highest value of spherical softness) has the highest activity [53]. It is well known that the interaction that will occur can occur in the part of the molecule where the local property of softness (S) has the highest value [54].

Although many parameters have been obtained from the calculations, few of the obtained parameters have visual representations. The parameters obtained from the visuals are given in Fig. 7. Here, the optimized structures of compounds are given in the first image. The second and third images show the locations of the HOMO and LUMO orbitals of the compounds. in the last image is the molecular electrostatic potential map of the compound. In this image, the red colored regions are the regions with the highest electron density. However, the blue colored regions are the regions with the lowest electron density [55].

Theoretical calculations are common methods used to compare the activities of compounds. The most used method among these calculations is molecular docking, which analyzes the interactions of compounds with various proteins in the calculations made by these methods. These interactions are generally chemical interactions [56]. As these interactions increase, it is seen that the activities of the compounds or their metal complexes increase. E total energy value of the calculated parameters of the studied compounds as a result of the calculations is a parameter used to compare the activities of the compounds [57]. It is known that the molecular activity with the most negative numerical value of this parameter is the highest. The interaction of molecules with proteins is very important. Because molecules enter the active centers of the proteins and interact with the proteins there, forming strong interactions with those proteins. In this way, they inhibit those proteins. therefore, the more interaction that molecule has with the protein, the more its activity increases. E total energy values of compounds calculated against various proteins are given in Table 7 and Figs. 8–9.

As a result of these molecular docking calculations, the activity of metal complex was compared. The chemical interactions occurring in this comparison cannot be seen in detail. Therefore, PLIP analysis was performed for more detailed analysis. When the activity comparison between ligand compounds and its metal complexes is made, it is seen that the activities of metal complexes are higher than ligand compounds [58–61]. Many studies support this situation. PLIP analysis of it was performed, the interactions of ligand and its metal complexes with this analysis are given in Tables 8–11.

In PLIP analysis, all chemical interactions of compounds are determined. The interaction pictures obtained as a result of this analysis are given in Figs. 10 and 11.

4. Conclusion

In this paper we have reported on the synthesis of two novel Schiff base derivatives and their copper (II) complexes. These Schiff base ligands, coordinated through the nitrogen atom of the azomethine moiety and the oxygen atom of the phenolic function, give the target complexes. The molecular structures of the ligands and complexes were characterized and confirmed by elemental analysis, FTIR, NMR (^{1}H and ^{13}C), molar conductance, UV–Vis, SEM and thermal analysis data.

It was found that these compounds were effective in MCF-7, HeLa cell lines at different levels. In addition, they had cytotoxic effects on normal L929 cells as well as cytotoxic effects on cancer cells. Considering the antioxidant investigation assays, these compounds generally caused low antioxidant and oxidative load in almost all cell lines, and therefore they did not change the oxidative stress index of all three cell lines. The results of the interactions between the compounds and pBR322 showed that these complexes were able to induce moderate conformational changes in DNA and DNA damage at higher doses. It was concluded that the compounds exhibited moderate antimicrobial activity against the target bacterial strains. Theoretical calculations were also performed to compare the ligands and complexes using the parameters obtained as a result of this calculation. The results indicated that the activities of the metal complexes are higher than those of the ligand compounds.

The addition of the trifluoromethyl (-CF_3) group to compounds has become increasingly popular and has served as a promising lead optimization strategy to improve protein–ligand interactions for biological investigations [62,63]. Previous studies have demonstrated that the

introduction of -CF_3 to specific ligand sites has led to the development of inhibitors in drug discovery studies [64,65]. In our study, since the positions of the CF_3 groups are fixed, and although these groups appear to be in the active site in molecular docking studies, it has been observed that there is no direct interaction with proteins. As can be seen from the docking results, the interactions were mostly through naphthol and phenol groups. Therefore, in order to better understand the effect of trifluoromethyl group on activity, it can be improved by changing its position and number.

CRediT authorship contribution statement

Arif Mermer: Conceptualization, Methodology, Software, Writing – original draft, Writing – review & editing, Visualization, Investigation. **Burak Tüzün:** Software, Writing – original draft, Visualization, Methodology. **Sevgi Durna Daştan:** Writing – original draft, Visualization, Methodology, Investigation. **Özge Çevik:** Writing – original draft, Visualization, Methodology, Investigation.

Declaration of Competing Interest

The authors declare that they have no known competing financial interests or personal relationships that could have appeared to influence the work reported in this paper.

Data availability

Data will be made available on request.

Acknowledgment

This work was supported by the Research Fund of TUBITAK ULAK-BIM High Performance and Grid Computing Center (TR-Grid e-Infrastructure).

Appendix A. Supplementary data

Supplementary data to this article can be found online at https://doi.org/10.1016/j.poly.2023.116487.

References

[1] Y. Guo, X. Hu, X. Zhang, X. Pu, Y. Wang, The synthesis of a Cu(II) Schiff base complex using a bidentate N2O2 donor ligand: crystal structure, photophysical properties, and antibacterial activities, RSC Adv. 9 (2019) 41737.

[2] D. Aggoun, M. Fernández-García, D. López, B. Bouzerafa, Y. Ouennoughi, F. Setifi, A. Ourari, New nickel (II) and copper (II) bidentate Schiff base complexes, derived from dihalogenated salicylaldehyde and alkylamine: Synthesis, spectroscopic, thermogravimetry, crystallographic determination and electrochemical studies, Polyhedron 187 (2020), 114640.

[3] a) Andiappan, K., Sanmugam, A., Deivanayagam, E., Karuppasamy, K., Kim, H. S., Vikraman, D. Schiff base rare earth metal complexes: Studies on functional, optical and thermal properties and assessment of antibacterial activity, International Journal of Biological Macromolecules, 124, 2019, 403-410; b) Demirci, S., Mermer, A., Ak, G., Aksakal, F., Colak, N., Demirbas, A., Ayaz, F. A., Demirbas, N. Conventional and Microwave-assisted Total Synthesis, Antioxidant Capacity, Biological Activity, and Molecular Docking Studies of New Hybrid Compounds, J. Heterocyclic Chem., 54, 2017, 1785- 1805.

[4] L.H. Abdel-Rahman, M.S.S. Adam, A.M. Abu-Dief, H. Moustafa, M.T. Basha, A. S. Aboraia, B.S. Al-Farhan, H.E. Ahmed, Synthesis, theoretical investigations, biocidal screening, DNA binding, in vitro cytotoxicity and molecular docking of novel Cu (II), Pd (II) and Ag (I) complexes of chlorobenzylidene Schiff base: Promising antibiotic and anticancer agents, Appl Organometal Chem. 32 (2018) e4527.

[5] A. Mermer, N. Demirbas, H. Uslu, A. Demirbas, S. Ceylan, Y. Sirin, Synthesis of novel Schiff bases using green chemistry techniques; antimicrobial, antioxidant, antiurease activity screening and molecular docking studies, J. Mol. Struct. 1181 (2019) 412–422.

[6] V.P. Daniel, B. Murukan, B.S. Kumari, K. Mohanan, Synthesis, spectroscopic characterization, electrochemical behaviour, reactivity and antibacterial activity of some transition metal complexes with 2-(N-salicylideneamino)-3-carboxyethyl-4,5-dimethylthiophene, Spectrochim. Acta A 70 (2008) 403–410.

[7] M. Revenga-Parra, T. Garcıa, E. Lorenzo, F. Pariente, Electrocatalytic oxidation of methanol and other short chain aliphatic alcohols on glassy carbon electrodes modified with conductive films derived from NiII-(N, N'-bis(2,5-dihydroxybenzylidene)-1,2-diaminobenzene), Sensor Actuat. B-Chem. 130 (2008) 730–738.

[8] Z. Messasma, A. Ourari, R. Mahdadi, S. Houchi, D. Aggoun, A. Kherbache, E. Bentouhami, Synthesis, spectral characterization, DFT computational studies and inhibitory activity of novel N2S2 tetradentates Schiff bases on metallobeta-lactamases of Acinetobacter baumannii, J. Mol. Struct. 1171 (2018) 672–681.

[9] T.L. Yusuf, S.D. Oladipo, S. Zamisa, H.M. Kumalo, I.A. Lawal, M.M. Lawal, N. Mabuba, Design of new schiff-base copper(II) complexes: synthesis, crystal structures, DFT study, and binding potency toward cytochrome P450 3A4, ACS Omega 6 (21) (2021) 13704–13718.

[10] X. Feng, J. Liu, DNA binding and in vitro anticarcinogenic activity of a series of new fashioned Cu(II)-complexes based on tricationic metalloporphyrin salicyloylhydrazone ligands, J. Inorg. Biochem. 178 (2018) 1–8.

[11] A. Ali, A. Ali, A. Tahir, M.A. Bakht, M.J. Ahsan, Ultrasound promoted green synthesis, anticancer evaluation, and molecular docking studies of hydrazines: a pilot trial, J. Enzyme Inhib. Med. Chem. 37 (1) (2022) 135–144.

[12] B.M. Essa, A.A. Selim, G.H. Sayed, K.E. Anwer, Conventional and microwave-assisted synthesis, anticancer evaluation, ^{99m}Tc-coupling and In-vivo study of some novel pyrazolone derivatives, Bioorg. Chem. 125 (2022), 105846.

[13] B.Z. Sibuh, S. Khanna, P. Taneja, P. Sarkar, N.K. Tanej, Molecular docking, synthesis and anticancer activity of thiosemicarbazone derivatives against MCF-7 human breast cancer cell line, Life Sci. 273 (2021), 119305.

[14] T. Dastan, U.M. Kocyigit, S. Durna-Dastan, P. Canturk-Kilickaya, P. Taslimi, O. Cevik, M. Koparir, C. Orek, I. Gulcin, A. Cetin, Investigation of acetylcholinesterase and mammalian DNA topoisomerases, carbonic anhydrase inhibition profiles, and cytotoxic activity of novel bis(α-aminoalkyl)phosphinic acid derivatives against human breast cancer, J. Biochem. Mol. Toxicol. 31 (11) (2017), e21971.

[15] O. Ertik, F. Danısman-Kalındemirtas, B. Kaya, R. Yanardag, S.E. Kuruca, O. Sahin, B. Ulkuseven, Oxovanadium(IV) complexes with tetradentate thiosemicarbazones. Synthesis, characterization, anticancer enzyme inhibition and in vitro cytotoxicity on breast cancer cells, Polyhedron 202 (2021), 115192.

[16] G.M. Brodeur, R. Iyer, J.L. Croucher, T. Zhuang, M. Higashi, V. Kolla, Therapeutic targets for neuroblastomas, Expert Opin. Ther. Targets 18 (2014) 277–292.

[17] M. Madakka, N. Jayaraju, N. Rajesh, Evaluating the antimicrobial activity and antitumor screening of green synthesized silver nanoparticles compounds, using Syzygium jambolanum, towards MCF7 cell line (Breast cancer cell line), J. Photochem. Photobiol. 6 (2021), 100028.

[18] A.D. Becke, Density-functional thermochemistry. I. The effect of the exchange-only gradient correction, J. Chem. Phys. 96 (3) (1992) 2155–2160.

[19] D. Vautherin, D.T. Brink, Hartree-Fock calculations with Skyrme's interaction. I. Spherical nuclei, Phys. Rev. C 5 (3) (1972) 626.

[20] E.G. Hohenstein, S.T. Chill, C.D. Sherrill, Assessment of the performance of the M05–2X and M06–2X exchange-correlation functionals for noncovalent interactions in biocompounds, J. Chem. Theory Comput. 4 (12) (2008) 1996–2000.

[21] R.S. Williams, R. Green, J.N. Glover, Crystal structure of the BRCT repeat region from the breast cancer-associated protein BRCA1, Nat. Struct. Biol. 8 (10) (2001) 838–842.

[22] U. Lücking, R. Jautelat, M. Krüger, T. Brumby, P. Lienau, M. Schäfer, G. Siemeister, The Lab Oddity Prevails: Discovery of Pan-CDK Inhibitor (R)-S-Cyclopropyl-S-(4-{[4-{[(1R, 2R)-2-hydroxy-1-methylpropyl] oxy}-5-(trifluoromethyl) pyrimidin-2-yl] amino} phenyl) sulfoximide (BAY 1000394) for the Treatment of Cancer, ChemMedChem 8 (7) (2013) 1067–1085.

[23] Adasme, M. F., Linnemann, K. L., Bolz, S. N., Kaiser, F., Salentin, S., Haupt, V. J., Schroeder, M. PLIP 2021: expanding the scope of the protein–ligand interaction profiler to DNA and RNA, Nucleic Acids Research, 49(W1), 2021, W530-W534.

[24] M. Al-Qubaisi, R. Rozita, S.K. Yeap, A.R. Omar, A.M. Ali, N.B. Alitheen, Selective cytotoxicity of goniothalamin against hepatoblastoma HepG2 cells, Compounds 16 (2011) 2944–2959.

[25] J.N. Eloff, A sensitive and quick microplate method to determine the minimal inhibitory concentration of plant extracts for bacteria, Planta Med. 64 (1998) 711–713.

[26] J. Figueiredo, J.L. Serrano, E. Cavalheiro, L. Keurulainen, J. Yli-Kauhaluoma, V. M. Moreira, S. Ferreira, F.C. Domingues, S. Silvestre, P. Almeida, Trisubstituted barbiturates and thiobarbiturates: Synthesis and biological evaluation as xanthine oxidase inhibitors, antioxidants, antibacterial and anti-proliferative agents, Eur. J. Med. Chem. 143 (2018) 829–842.

[27] O. Erel, A novel automated direct measurement method for total antioxidant capacity using a new generation, more stable ABTS radical cation, Clinical Biochem. 37 (4) (2004) 277–285.

[28] O. Erel, A new automated colorimetric method for measuring total oxidant status, Clinical Biochem. 38 (12) (2008) 1103–1111.

[29] C. Bogatarkan, S. Utku, L. Acik, Synthesis, characterization and pBR322 plasmid DNA interaction of platinum (II) complexes with imidazole and 2-phenylimidazole as carrier ligands, Rev. Roum. Chim. 60 (1) (2015) 59–64.

[30] Dennington, R., Keith, T. A., Millam, J. M. GaussView 6.0. 16. Semichem Inc., Shawnee Mission, 2016, KS, USA.

[31] Frisch M. J., Trucks G. W., Schlegel H. B., Scuseria G. E., Robb M. A., Cheeseman J. R., Scalmani G., Barone V., Mennucci B., Petersson G. A., Nakatsuji H., Caricato M., Li X., Hratchian H. P., Izmaylov A. F., Bloino J., Zheng G., Sonnenberg J. L., Hada M., Ehara M., Toyota K., Fukuda R., Hasegawa J., Ishida M., Nakajima T., Honda Y., Kitao O., Nakai H., Vreven T., Montgomery J. A., Peralta J. E., Ogliaro F., Bearpark M., Heyd J. J., Brothers E., Kudin K. N., Staroverov V. N., Kobayashi R.,

Normand J., Raghavachari K., Rendell A., Burant J. C., Iyengar S. S., Tomasi J., Cossi M., Rega N., Millam J. M., Klene M., Knox J. E., Cross J. B., Bakken V., Adamo C., Jaramillo J., Gomperts R., Stratmann R. E., Yazyev O., Austin A. J., Cammi R., Pomelli C., Ochterski J. W., Martin R. L., Morokuma K., Zakrzewski V. G., Voth G. A., Salvador P., Dannenberg J. J., Dapprich S., Daniels A. D., Farkas O., Foresman J. B., Ortiz J. V., Cioslowski J., Fox D. J. Gaussian 09, revision D.01. Gaussian Inc, 2009, Wallingford CT.

[32] E. Onem, B. Tuzun, S. Akkoc, Anti-quorum sensing activity in Pseudomonas aeruginos a PA01 of benzimidazolium salts: electronic, spectral and structural investigations as theoretical approach, J. Biomol. Struct. Dyn. 40 (15) (2022) 6845–6856.

[33] M. Tapera, H. Kekecmuhammed, B. Tuzun, E. Sarıpınar, U.M. Kocyigit, E. Yıldırım, Y. Zorlu, Synthesis, carbonic anhydrase inhibitory activity, anticancer activity and molecular docking studies of new imidazolyl hydrazone derivatives, J. Mol. Struct. 1269 (2022), 133816.

[34] G. Kurtoglu, B. Avar, H. Zengin, M. Kose, K. Sayin, M. Kurtoglu, A novel azo-azomethine based fluorescent dye and its Co(II) and Cu(II) metal chelates, J. Mol. Liq. 200 (2014) 105–114.

[35] D. Ritchie, T.H. Orpailleur, Protein docking using spherical polar fourier correlations copyright c, User Manual. 8 (2013).

[36] D.W. Ritchie, V. Venkatraman, Ultra-fast FFT protein docking on graphics processors, Bioinformatics (Oxford, England) 26 (19) (2010) 2398–2405.

[37] M.D. Awouafack, L.J. McGaw, S. Gottfried, R. Mbouangouere, P. Tane, M. Spiteller, J.N. Eloff, Antimicrobial activity and cytotoxicity of the ethanol extract, fractions and eight compounds isolated from Eriosema robustum (Fabaceae), BMC Complement. Altern. Med. 13 (2013) 289.

[38] A. Mermer, S. Alyar, Synthesis, characterization, DFT calculation, antioxidant activity, ADMET and molecular docking of thiosemicarbazide derivatives and their Cu (II) complexes, Chem. Biol. Interact. 351 (2022), 109742.

[39] Singh, K., Kumar, Y., Puri, P., Sharma, C., Aneja, K. R. Antimicrobial, spectral and thermal studies of divalent cobalt, nickel, copper and zinc complexes with triazole Schiff bases, Arab. J. Chem. 2017, 10, S978-S987.

[40] J. Devi, M. Yadav, D. Kumar, L.S. Naik, D.K. Jindal, Some divalent metal(II) complexes of salicylaldehyde-derivedSchiff bases: Synthesis, spectroscopic characterization, antimicrobial andin vitroanticancer studies, Appl. Organometal. Chem. 33 (2019) e4693.

[41] R.R. Randle, D.H. Whiffen, The characteristic infrared absorption frequencies of aromatic trifluuromethyl compounds, J. Chem. Soc. 1311–1313 (1955).

[42] M. Gaber, K. El-Baradie, N. El-Wakiel, S. Hafez, Synthesis and characterization studies of 3-formyl chromone Schiff base complexes and their application as antitumor, antioxidant and antimicrobial, Appl. Organometal. Chem. 34 (2020) e5348.

[43] H. Boulebd, Y. Zine, I.A. Khodja, A. Mermer, A. Demir, A. Debache, Synthesis and radical scavenging activity of new phenolic hydrazone/hydrazide derivatives: Experimental and theoretical studies, J. Mol. Struct. 1249 (2022), 131546.

[44] P.B. Tchounwou, C. Newsome, J. Williams, K. Glass, Copper-induced cytotoxicity and transcriptional activation of stress genes in human liver carcinoma (HepG2) cells, Met Ions Biol Med. 10 (2008) 285–290.

[45] Cortizo, M.C., Lorenzo De Mele, M.F. Cytotoxicity of copper ions released from metal variation with the exposure period and concentration gradients. Biological Trace Element Research, 102, 2004, 0129.

[46] R. Çakmak, E. Başaran, M. Boğa, Ö. Erdoğan, E. Çınar, Ö. Çevik, Schiff base derivatives of 4-aminoantipyrine as promisingmolecules: synthesis, structural characterization, and biological activities, Russ. J. Bioorg. Chem. 48 (2) (2022) 334–344.

[47] V. Kuete, Potential of Cameroonian plants and derived products against microbial infections: a review, Planta Med. 76 (14) (2010) 1479–1491.

[48] D. Wang, S.J. Lippard, Cellular processing of platinum anticancer drugs, Nat. Rev. Drug Discov. 4 (2005) 307–320.

[49] A.M. Abu-Dief, L.H. Abdel-Rahman, A.A. Abdelhamid, A.A. Marzouk, M. R. Shehata, M.A. Bakheet, O.A. Almaghrabi, A. Nafady, Synthesis and characterization of new Cr(III), Fe(III) and Cu(II) complexes incorporating multi-substituted aryl imidazole ligand: structural, DFT, DNA binding, and biological implications, Spectrochim. Acta Part A 228 (2020), 117700.

[50] A. Mermer, M.V. Bulbul, S.M. Kalender, I. Keskin, B. Tuzun, O.E. Eyupoglu, Benzotriazole-oxadiazole hybrid compounds: synthesis, anticancer activity, molecular docking and ADME profiling studies, J. Mol. Liq. 359 (2022), 119264.

[51] Z. Garda, E. Molnár, N. Hamon, J.L. Barriada, D. Esteban-Gómez, B. Váradi, V. Nagy, K. Pota, F.K. Kálmán, I. Tóth, N. Lihi, C. Platas-Iglesias, E. Tóth, R. Tripier, G. Tircsó, Complexation of Mn(II) by rigid pyclen diacetates: equilibrium, kinetic, relaxometric, density functional theory, and superoxide dismutase activity studies, Inorg. Chem. 60 (2021) 1133–1148.

[52] S. Kaya, B. Tüzün, C. Kaya, I.B. Obot, Determination of corrosion inhibition effects of amino acids: quantum chemical and molecular dynamic simulation study, J. Taiwan Inst. Chem. Eng. 58 (2016) 528–535.

[53] M. Rbaa, M. Galai, E. Berdimurodov, B. Tüzün, M.E. Touhami, A. Zarrouk, A. Elgendy, Novel bio-based green and sustainable corrosion inhibitors: development, characterization, and corrosion inhibition applications, Handbook of Research on Corrosion Sciences and Engineering (2023) 343–361.

[54] Ş. Erdoğan, B. Tüzün, Relationship between the chemical structure and the corrosion inhibition properties of some organic molecules: challenges and industrial applications, Handbook of Research on Corrosion Sciences and Engineering (2023) 42–64.

[55] G. Sarkı, B. Tuzun, D. Unluer, H. Kantekin, Synthesis, characterization, chemical and biological activities of 4-(4-methoxyphenethyl)-5-benzyl-2-hydroxy-2H-1,2,4-triazole-3 (4H)-one phthalocyanine derivatives, Inorg. Chim. Acta (2022), 121113.

[56] H. Kekecmuhammed, M. Tapera, B. Tuzun, S. Akkoc, Y. Zorlu, E. Sarıpınar, Synthesis, molecular docking and antiproliferative activity studies of a thiazole-based compound linked to hydrazone moiety, ChemistrySelect 7 (26) (2022), e202201502.

[57] D. Majumdar, J.E. Philip, B. Tüzün, A. Frontera, R.M. Gomila, S. Roy, K. Bankura, Unravelling the synthetic mimic, spectroscopic insights, and supramolecular crystal engineering of an innovative heteronuclear Pb (II)-salen cocrystal: an integrated DFT, QTAIM/NCI Plot, NLO, molecular docking/PLIP, and antibacterial appraisal, J. Inorg. Organomet. Polym Mater. 32 (2022) 4320–4339.

[58] S. Grimme, Exploration of chemical compound, conformer, and reaction space with meta-dynamics simulations based on tight-binding quantum chemical calculations, J. Chem. Theory Comput. 15 (5) (2019) 2847–2862.

[59] A. Günsel, A.T. Bilgiçli, B. Tüzün, H. Pişkin, M.N. Yarasir, B. Gündüz, Optoelectronic parameters of peripherally tetra-substituted copper (II) phthalocyanines and fabrication of a photoconductive diode for various conditions, New J. Chem. 44 (2) (2020) 369–380.

[60] A. Günsel, A.T. Bilgiçli, H. Pişkin, B. Tüzün, M.N. Yarasir, B. Gündüz, Synthesis of non-peripherally tetra-substituted copper (II) phthalocyanines: characterization, optical and surface properties, fabrication and photo-electrical properties of a photosensitive diode, Dalton Trans. 48 (39) (2019) 14839–14852.

[61] A.T. Bilgicli, H.G. Bilgiçli, A. Günsel, H. Pişkin, B. Tüzün, M.N. Yarasir, M. Zengin, The new ball-type zinc phthalocyanine with SS bridge; Synthesis, computational and photophysicochemical properties, J. Photochem. Photobiol. A Chem. 389 (2020), 112287.

[62] R. Buratto, D. Mammoli, E. Canet, G. Bodenhausen, Ligand protein affinity studies using long-lived states of fluorine-19, nuclei, J. Med. Chem. 59 (2016) 1960–1966.

[63] J.B.I. Sap, N.J.W. Straathof, T. Knauber, C.F. Meyer, M. Medebielle, L. Buglioni, C. Genicot, A.A. Trabanco, T. Noel, C.W. Am Ende, V. Gouverneur, Organophotoredox hydrodefluorination of trifluoromethylarenes with translational applicability to drug discovery, J. Am. Chem. Soc. 142 (2020) 9181–9187.

[64] Y. Zafrani, D. Yeffet, G. Sod-Moriah, A. Berliner, D. Amir, D. Marciano, E. Gershonov, S. Saphier, Difluoromethyl bioisostere: examining the "lipophilic hydrogen bond donor concept, J. Med. Chem. 60 (2017) 797–804.

[65] A.M.S. Riel, D.A. Decato, J. Sun, C.J. Massena, M.J. Jessop, O.B. Berryman, The intramolecular hydrogen bonded-halogen bond: a new strategy for preorganization and enhanced binding, Chem. Sci. 9 (2018) 5828–5836.